International Ocean Discovery Program

Expedition 388 Scientific Prospectus

Equatorial Atlantic Gateway: origin, evolution, and paleoenvironment of the Equatorial Atlantic Gateway

Tom Dunkley Jones
Co-Chief Scientist
School of Geography, Earth and Environmental Science
University of Birmingham
United Kingdom

Gerson Fauth
Co-Chief Scientist
Instituto Tecnológico de Micropaleontologia
Universidade do Vale do Rio dos Sinos
Brazil

Leah J. LeVay
Expedition Project Manager/Staff Scientist
International Ocean Discovery Program
Texas A&M University
USA

IODP
INTERNATIONAL OCEAN DISCOVERY PROGRAM

Publisher's notes

This publication was prepared by the *JOIDES Resolution* Science Operator (JRSO) at Texas A&M University (TAMU) as an account of work performed under the International Ocean Discovery Program (IODP). Funding for IODP is provided by the following international partners:

National Science Foundation (NSF), United States
Ministry of Education, Culture, Sports, Science and Technology (MEXT), Japan
European Consortium for Ocean Research Drilling (ECORD)
Ministry of Science and Technology (MOST), People's Republic of China
Korea Institute of Geoscience and Mineral Resources (KIGAM)
Australia-New Zealand IODP Consortium (ANZIC)
Ministry of Earth Sciences (MoES), India
Coordination for Improvement of Higher Education Personnel (CAPES), Brazil

Portions of this work may have been published in whole or in part in other IODP documents or publications.

This IODP *Scientific Prospectus* is based on precruise *JOIDES Resolution* Facility advisory panel discussions and scientific input from the designated Co-Chief Scientists on behalf of the drilling proponents. During the course of the cruise, actual site operations may indicate to the Co-Chief Scientists, the Staff Scientist/Expedition Project Manager, and the Operations Superintendent that it would be scientifically or operationally advantageous to amend the plan detailed in this prospectus. It should be understood that any proposed changes to the science deliverables outlined in the plan presented here are contingent upon the approval of the IODP JRSO Director.

Disclaimer

Copyright

Citation

Dunkley Jones, T., Fauth, G., and LeVay, L.J., 2019. *Expedition 388 Scientific Prospectus: Equatorial Atlantic Gateway.* International Ocean Discovery Program. https://doi.org/10.14379/iodp.sp.388.2019

ISSN

World Wide Web: 2332-1385

June 2019

Abstract

International Ocean Discovery Program (IODP) Expedition 388 seeks to answer first-order questions about the tectonic, climatic, and biotic evolution of the Equatorial Atlantic Gateway (EAG). The scheduled drilling operations will target sequences of Late Cretaceous and Cenozoic sediments offshore northeast Brazil, just south of the theorized final opening point of the EAG. These sequences are accessible to conventional riserless drilling in the vicinity of the Pernambuco Plateau, part of the northeastern Brazilian continental shelf. This region was chosen to satisfy two key constraints: first, that some of the oldest oceanic crust of the equatorial Atlantic and overlying early postrift sediments are present at depths shallow enough to be recovered by riserless drilling, and second, Late Cretaceous and Paleogene sediments preserved on the Pernambuco Plateau are close enough to the continental margin and at shallow enough paleowater depths (<2000 m) to provide well-preserved organic biomarkers and calcareous microfossils for multiproxy studies of greenhouse climate states. New records in this region will allow us to address major questions in four key objectives: the early rift history of the equatorial Atlantic, the biogeochemistry of the restricted equatorial Atlantic, the long-term paleoceanography of the EAG, and the limits of tropical climates and ecosystems under conditions of extreme warmth. Tackling these major questions with new drilling in the EAG region will advance our understanding of the long-term interactions between tectonics, oceanography, ocean biogeochemistry, and climate and the functioning of tropical ecosystems and climate during intervals of extreme warmth.

Schedule for Expedition 388

International Ocean Discovery Program (IODP) Expedition 388 is based on IODP drilling Proposal 864-Full2 and 864-Add (available at **http://iodp.tamu.edu/scienceops/expeditions/equatorial_atlantic_gateway.html**). Following evaluation by the IODP Scientific Advisory Structure, the expedition was scheduled for the research vessel (R/V) *JOIDES Resolution*, operating under contract with the *JOIDES Resolution* Science Operator (JRSO). At the time of publication of this *Scientific Prospectus*, the expedition is scheduled to start in Recife, Brazil, on 26 June 2020 and to end in Recife, Brazil, on 26 August. A total of 61 days will be available for the transit, drilling, coring, and downhole measurements described in this report (for the current detailed schedule, see **http://iodp.tamu.edu/scienceops**). Further details about the facilities aboard *JOIDES Resolution* can be found at **http://iodp.tamu.edu/publicinfo/drillship.html**.

Introduction

Background

Recovery of extended sequences of Cretaceous and Paleogene sediments from the vicinity of the Pernambuco Plateau, northeast Brazil (Figures **F1**, **F2**), will provide a unique record of equatorial Atlantic tectonic, climatic, and biotic evolution stretching back an estimated 100 My or more. Extending back to the final phases of the breakup of Gondwana, recovery of new sedimentary sequences would provide unique records from the early rifting of a supercontinent through the final opening of the Equatorial Atlantic Gateway (EAG) and the transition to a fully modern system of ocean circulation. The new records would also allow us to constrain the relationships between tectonics and rifting processes and the associated sedimentary, biogeochemical, and paleoclimate phenomena in adjacent ocean basins. Sediments from the Pernambuco Plateau would also provide a very long time series of Late Cretaceous to modern tropical paleoclimates because of the relatively small latitudinal movement of this location since the Early Cretaceous (Müller et al., 2016). The Pernambuco Plateau is the only location yet identified along the tropical Brazilian continental margin where sediments from the Late Cretaceous supergreenhouse epochs are accessible within reach of riserless drilling.

Constraining the tectonic and early rift evolution of the EAG is critical for testing geodynamic models of South Atlantic rifting and passive margin development and hypotheses relating the evolution of the EAG to interhemispheric oceanic exchange and global climate via oceanic heat redistribution (MacLeod et al., 2011; Voigt et al., 2013). The proposed drilling locations are situated at the northern end of an evolving rift system in which massive evaporitic sequences were deposited during the Aptian (Tedeschi et al., 2017) and whose termination is likely controlled by the evolution of the Atlantic rift system and widening of critical oceanic gateways. The final restriction to oceanic exchange through the EAG "transform pinch point" is thought to be the Ghanaian Ridge at the Romanche fracture zone (FZ) (Granot and Dyment, 2015; Heine et al., 2013) (Figure **F3**) north of the Pernambuco Plateau. During the Early Cretaceous, this topographic high isolated the large deep basins of the South Atlantic from Central/equatorial Atlantic waters. Here, this pinch point will be regarded as the central point of the EAG, with the basins north and west of this referred to as the "equatorial Atlantic" and south of this— including the Pernambuco Plateau—as the "equatorial South Atlantic." Past Ocean Drilling Program (ODP) legs recovered organic-rich Late Cretaceous successions from both the eastern (Cote d'Ivoire-Ghana transform continental margin; ODP Leg 159) and western (Demerara Rise; ODP Leg 207) margins of the equatorial Atlantic but only north of the EAG (Figure **F4**). As a result, little is known about the Late Cretaceous–Paleogene environments in the equatorial South Atlantic or about the history of water mass exchange between the South and equatorial Atlantic. Expedition 388 aims to address this data gap with new ocean drilling directly in the equatorial South Atlantic.

Hydrocarbon exploration in the South Atlantic has discovered major Early Cretaceous depocenters of organic carbon and evaporite sequences, typically capped by thick postrift successions (Davison, 2007). However, apart from Deep Sea Drilling Project (DSDP) Sites 356 (São Paulo Plateau; The Shipboard Scientific Party, 1977) and 530 (Angola Basin; Shipboard Scientific Party, 1984), there has been no direct recovery of organic-rich Cretaceous sediments during DSDP, ODP, or IODP operations in the South Atlantic. Key questions thus remain about the nature of organic carbon burial, biogeochemistry, and oceanography of the Cretaceous South Atlantic and its similarity or differences from the equatorial Atlantic system. There is great potential for records of these warm and low-oxygen oceanic systems to provide a natural laboratory to constrain the impact of extreme conditions on marine ecosystems, nutrient cycling, and climate feedbacks (Jenkyns, 2010; Tedeschi et al., 2017). Expedition 388 also seeks to recover long successions of clay-rich hemipelagic sediments from the northeast Brazil continental margin to extract high-quality climate proxy data to determine tropical climate evolution over the past 100 My. New scientific ocean drilling in the vicinity of the Pernambuco Plateau will recover key new records of South Atlantic basin evolution and the tropical climate system to address these questions.

Geological setting

The Pernambuco Plateau is an extension of thinned continental crust that forms the marginal Pernambuco Basin, extending from the narrow continental shelf of northeast Brazil out to water depths of 4000 m (Figure **F5**). Site survey work undertaken in preparation for this proposal has shown that this plateau is actually a complex of crustal-scale tilted fault blocks bounding very deep north-northeast– to south-southwest–trending rift basins, some with 6 km or more of synrift sediment fill including large salt bodies previously thought to be absent from the northeast Brazilian margin and multiple volcanic edifices (Buarque et al., 2016). The plateau is located immediately south of the east-west–trending Pernambuco shear zone (PESZ), a major pre-Cambrian shear zone that reactivated during the Cretaceous (Figure **F2**). The deep rift basins of the inner plateau appear to terminate against this structure with basement present at shallow depths north of the plateau. To the south, basins in the Pernambuco Plateau terminate against the Maragogi-Barreiros high, which separates these basins from the Alagoas Basin.

Within the Pernambuco Plateau are two distinct basement highs: the east-west–trending Gaibu high near the center of the plateau and the Itamaracá high, which trends northwest–southeast on the northeast border of the plateau (Figure **F5**). Regional airborne gravity (Figure **F6**) and magnetic surveys, integrated with industry seismic data studied for this proposal, support the suggestion that these two distinct highs represent magmatic centers within the plateau (Buarque et al., 2016). Upper Albian volcanics (102–103 Ma), the Ipojuca magmatic suite, are present on the onshore portion of the Pernambuco Basin (Buarque et al., 2016). Extrusive and intrusive volcanics observed offshore in the seismic data are clearly postrift (Buarque et al., 2016). Similar volcanic systems in the offshore Sergipe-Alagoas Basin have also been dated to the late Albian (104 Ma; Caixeta et al., 2014). Primary Site PER-9B is planned to penetrate into and recover volcanic material for dating and compositional analysis from one of these volcanic edifices on the outer margin of the plateau.

Seismic studies/site survey data

Site identification and characterization are based on the 2009–2011 BrasilSpan seismic reflection data set, provided by industrial partner ION Geophysical (Figure **F5**). BrasilSpan lines image the entire sedimentary succession and crustal basement, well deeper than our target drill depth (<1.5 km) and with a vertical stratigraphic resolution of 5–10 m across the drilling target intervals. Acquisition and resolution specifications all meet or exceed IODP idealized survey parameters: 10.2 km source-receiver offsets, 12.5 m common midpoint (CMP) interval, 102 fold, ~50 Hz dominant frequency at target depth, and 2 ms sampling rate. ION's source and processing design give excellent resolution and signal-to-noise characteristics with true amplitude processing. Prestack time migration (PSTM) sections and prestack depth migration (PSDM) data, stacking velocities, PSTM and PSDM velocity models, and navigation data files of relevant lines, as well as acquisition and processing reports, are available from the IODP Site Survey Data Bank (SSDB). This supporting site survey data have been made available to IODP only for the purposes of Expedition 388 operations. These data remain proprietary; access and use by individual science participants requires their own direct nondisclosure agreements with ION.

Additional near-seabed data sets

As part of the site survey project, all available single and multibeam bathymetry available across the Pernambuco Plateau has been collated, including original ship track data from Brazilian national databases and the National Oceanic and Atmospheric Administration (NOAA) National Geophysical Data Center (NGDC). These data have been quality checked and interpolated to produce the best publicly available bathymetry for the Pernambuco Plateau (Figure **F5**). In addition, SeaSeep, an independent Brazil-based geophysical survey company, has a 15 m resolution multibeam bathymetric survey of Pernambuco Plateau that covers proposed drill sites on the plateau. For these locations, SeaSeep has provided additional bathymetric data around each site location.

Stratigraphic model and well ties

To date, there has been no commercial or scientific ocean drilling anywhere on the Pernambuco Plateau, which is truly a frontier area for both academic and industrial investigation. Two types of well-log correlation are, in theory, possible: medium-distance (50–100 km) updip correlation involving projection from coastal seismic sections to onshore wells close to the coast and long-distance (several 100 km) along-strike correlation with commercial wells drilled further along the margin. Onshore wells in the vicinity of Recife have recovered hundreds of meters of Late Cretaceous siliciclastic sediments, but these are in an inner rift system that is isolated from the plateau stratigraphy. Instead, we used a combination of BrasilSpan and Brazil Navy (LEPLAC Program) seismic surveys for a long-range along-strike stratigraphic correlation to industry wells in the Alagoas Basin. Because of the bounding Maragogi-Barreiros high south of the Pernambuco Plateau, this well tie had to be made by tracing stratigraphy out into deep water east of the plateau, then south, and finally back into the appropriate well ties on the continental margin of the Alagoas Basin. There is considerable uncertainty in this well tie, and so local seismic constraints, such as the position of oceanic or volcanic basement and the identification of the syn- to postrift transition, provide more useful information on the stratigraphy of drilling targets. Full logs of the wells (1-ALS-42 and 1-ALS-32) and data for the seismic lines used for this tie have been uploaded with the site survey package.

Scientific objectives

The the following key science questions can uniquely be addressed by Expedition 388 recovery of Cretaceous–Paleogene volcanic and sedimentary sequences on the Pernambuco Plateau.

1. *Early rift history of the equatorial Atlantic (Sites PER-4A, PER-7A, PER-11A)*

Localization of rifting, passive margin formation, and magmatism

During the Late Jurassic and Early Cretaceous, the Pernambuco Plateau was located at the confluence of three major intracontinental rift systems whose development eventually led to the breakup of the supercontinent Gondwana (Heine et al., 2013; Heine and Brune, 2014). In a relatively short time (~5–10 Ma), changes in overall plate configuration generated more than 15,000 km of new extensional plate boundaries along the South/equatorial Atlantic and west/central African rifts. Simple two-plate kinematic models of the South

Atlantic rift have proven to be inadequate to resolve the early phases of extension, especially where there was significant deformation in intraplate basins around this failed triple-junction system (Darros de Matos, 1999; Marques et al., 2014; Valença et al., 2003). New kinematic modeling is able to apportion the degree of extension accommodated within intraplate basins and the final rift breakup (Heine et al., 2013), but the absolute timing of this switch in rift dynamics and hence predicted relative extension rates are poorly constrained (Heine and Brune, 2014). Although the final breakup between the African Kwanza/Benguela basin segment and the Brazilian Santos Basin margin is thought to be latest Aptian (~115–112 Ma; Heine et al., 2013; Torsvik et al., 2009), the effect of the diachronism generated by north-forward rift propagation is still unknown for the northernmost South Atlantic.

Plate kinematic models of the South Atlantic opening provide self-consistent realizations of plate movements, oceanic crustal age, and spreading rates through time. These models are constructed using plate rotation poles, along with some analysis of intraplate deformation, and can be constrained against available seafloor magnetic isochrons (Heine et al., 2013; Heine and Brune, 2014). However, most of the geological data behind these models are from the continental realm, whereas the models make predictions about the long-term evolution of oceanic basins. These predictions involve inherent model assumptions about the rates and magnitude of intraplate deformation and the apportionment of divergence between continental and oceanic realms. For the early stages of northern South Atlantic and equatorial Atlantic rifting, independent constraints on these model predictions of seafloor spreading are almost entirely absent because of the absence of seafloor magnetic isochrons in the Cretaceous Normal Superchron (CNS; Granot and Dyment, 2015) (Figure **F1**). Recent work, however, based on reanalysis of continental rotation poles proposes a significantly later breakup age for the equatorial South Atlantic, closer to the Albian/Cenomanian boundary (~100 Ma) (Pérez-Díaz and Eagles, 2017a, 2017b). Distinguishing between these divergent models will be a major objective of Expedition 388 through direct dating of the oldest oceanic crust and through the characterization of Albian–Cenomanian successions and whether they represent nascent early postrift successions (Pérez-Díaz and Eagles, 2017a, 2017b) or a well-established mature oceanic system with deep (~4000 m) water sedimentation (Heine and Brune, 2014; Heine et al., 2013; Müller et al., 2008) (Figure **F7**). Robust and temporally well-constrained models of rifting are fundamental to an improved understanding of the process of triple junction evolution into passive margin conjugate pairs. In the equatorial Atlantic and equatorial South Atlantic, the tectonic evolution of this system is also especially important because of its controlling impact on Atlantic oceanography and global biogeochemical cycles (Tedeschi et al., 2017; see below).

In either scenario, Expedition 388 aims to recover a marine stratigraphic record spanning large portions of the Aptian to Santonian CNS (Chron C34n) (Granot and Dyment, 2015; Heine et al., 2013; Moulin et al., 2010). Although new deep-tow magnetic surveys may provide some constraints in the CNS using field strength variations (Granot and Dyment, 2015; Granot et al., 2012), direct integration of biostratigraphic and radiometric dating in the CNS will be valuable for improved chronostratigraphies. Along most of the African-American conjugate margin, postrift sediments of this age are buried under a thick sedimentary sequence (>2 km), making them inaccessible to riserless drilling and increasing the value of new stratigraphic records of this interval from the Pernambuco region. Further, the presence of magmatic systems close to the syn- to postrift transition, as observed in seismic surveys of the Pernambuco Plateau, present the possibility of recovering volcanic material in the sedimentary sequence spanning parts of the CNS. Together with biostratigraphic data, the dating of this volcanic or volcaniclastic material has the potential to provide substantially improved chronostratigraphic constraints in the CNS as well as a detailed temporal framework for the science objectives of Expedition 388. Biostratigraphic correlations and dating of Early Cretaceous South Atlantic nonmarine synrift and early postrift has been achieved using ostracods (Poropat and Colin, 2012) and palynology (Regali and Santos, 1999). In early postrift marine strata, blooms of shallow-dwelling planktonic foraminiferal species are characteristic and age diagnostic (Koutsoukos, 1992; Koutsoukos et al., 1989), and there are well-established South Atlantic dinoflagellate zonations (Arai, 2014; Arai and Botelho Neto, 1996). Where possible, this will be tied into global schemes with standard calcareous nannofossil biostratigraphy.

Early rift environments and the transition to oceanic conditions

Expedition 388 sampling of early postrift sedimentary successions will provide uniquely detailed records of the young equatorial South Atlantic environments during extreme oceanic and climatic conditions. Early postrift deposits may be contemporaneous with the later stages of major evaporite sequences of the South Atlantic basins. In regional seismic data, there is no indication of salt deposition above oceanic crust in the deep-water equatorial South Atlantic, implying that early postrift deposits may be more similar to Aptian terrestrial and lacustrine facies of the South Atlantic (Davison, 2007). If the final equatorial South Atlantic breakup is later, in the late Albian or Cenomanian, then these postrift successions will likely be fully marine throughout. In either case, the recovery of these early postrift sequences will provide major new insights into the depositional environments of the early rift system lacustrine and/or marine waters, the nature of authigenic and biogenic carbonates and chemical precipitates, the provenance of early rift sediments and the nature of the sediment routing systems that delivered them, and the extent and nature of organic carbon burial. Based on existing seismic data, we infer that primary Site PER-4A and alternate Site PER-7A are located close to the continent–ocean transition on the oldest oceanic crust adjacent to the continental margin.

By the early Aptian (~119–118 Ma), plate kinematic models predict that the southern equatorial Atlantic Ocean basin had reached a size comparable to the present-day Red Sea. Along the equatorial Atlantic, continued strike-slip deformation along long-offset oceanic transform faults with high relief, such as the Ghanaian Ridge at the Romanche fracture zone (Granot and Dyment, 2015), led to the development of isolated passive margin segments and deep basins until final breakup was achieved at ~105 Ma (Heine and Brune, 2014; Heine et al., 2013). Postrift sedimentary sequences recovered off the Pernambuco Plateau are ideally placed to record (1) the transition to full marine conditions with oceanic exchange across the southern South Atlantic and into the Southern Ocean via the Walvis Ridge system and (2) the gradual opening and exchange between the highly restricted and localized basins of the equatorial Atlantic and the South Atlantic. Such a progression will leave a strong signal in the sedimentology, geochemistry, and fossil content of the successions recovered from Sites PER-4A, 7A, and/or 11A. Water mass tracers as well as paleodepth and paleoredox indicators will be used to determine the timing and rate of basin evolution across both the South and equatorial Atlantic and the subsidence history of the equatorial Atlantic (Figure **F8**).

2. *Biogeochemistry of the hydrographically restricted Equatorial South Atlantic*

How did the hydrographically restricted equatorial South Atlantic interact with global biogeochemical cycles in the Cretaceous?

The evolution, radiation, and extinction of marine life is intimately linked to the cycling of bioessential macro- and micronutrients and the associated variability in seawater redox and pH (e.g. Jenkyns, 2010; Lyons et al., 2014). Hydrographically restricted marine basins exert a disproportionately large influence on modern global biogeochemical cycling because of their propensity to remove large quantities of redox-sensitive bioessential metals such as zinc, molybdenum, and iron from the water column and into sulfidic seafloor sediments. The expansion and contraction of such environments over time can exert strong control on the composition of marine biota (e.g. Owens et al., 2016), sites of organic carbon burial, the global carbon cycle, atmospheric CO_2 levels, and climate (e.g. Falkowski, 1997; Keeling et al., 2010; Tedeschi et al., 2017). In the modern system with low sea levels and wide ocean basins ventilated by high-latitude deep-water production, the impact of restricted basins is more limited. During the warm climates of the Cretaceous with reduced deep-water ventilation, the biogeochemistry of the narrow, young Central and South Atlantic Ocean was likely a major source and sink in redox-sensitive global biogeochemical cycles. Tracing the geographical extent, character, and evolution of this early rift Atlantic system is critical for understanding the links between ocean chemistry, marine ecosystems, and the global climate system (Tedeschi et al., 2017).

Late Cretaceous paleoenvironments of the Central Atlantic are constrained by existing ODP records from Leg 207 (Demerara Rise) on the western margin and Leg 159 (Deep Ivorian Basin) on the eastern margin; however, both of these locations are north of the EAG and cannot be used to constrain marine conditions in the equatorial South Atlantic. They do, however, provide a good characterization of Central Atlantic water mass chemistry (e.g., Jiménez Berrocoso et al., 2010), which can be used as a marker for water mass exchange into the equatorial South Atlantic if new records were recovered from this region. Sediment records from the equatorial Atlantic Ocean indicate sustained organic-rich shale deposition from the Cenomanian to the Campanian. This has been explained by restricted intermediate and deep-water ventilation (e.g. Wagner, 2002; Friedrich and Erbacher, 2006), potentially enhanced by upwelling-driven productivity along the southern margin of the proto-North Atlantic Ocean (Trabucho-Alexandre et al., 2012). In contrast, the marine environments of the equatorial South Atlantic during the Late Cretaceous are largely unknown. The presence of large salt basins in the central South Atlantic, extensively characterized by industry, indicates that a hydrographically restricted regime prevailed during the Early Cretaceous. The Cretaceous environments of the youngest and most restricted equatorial South Atlantic basins are, however, poorly known and have the potential for poor ventilation and warm ocean temperatures to drive this system into similar low-oxygen/high-organic carbon burial conditions as the equatorial Atlantic. Modeling studies (e.g., Handoh et al., 1999; Monteiro et al., 2012) predict exactly such conditions in the proto-South Atlantic prior to the full opening and deepening of the EAG. A major aim of this proposal is to groundtruth these predictions by constraining the spatial and temporal extent of organic-rich deposition in the equatorial South Atlantic.

In addition to tectonic restriction of the equatorial South Atlantic, oceanographic and climate conditions may have substantially modulated the spatial patterns, extent, and nature of organic carbon deposition through the Late Cretaceous. First, high-nutrient, low-oxygen water masses might have been exported southward over the EAG, enhancing productivity and carbon burial in the equatorial South Atlantic. Such processes occur adjacent to modern systems with restricted hydrographic conditions (Savchuk and Wulff, 2009; Slomp et al., 2013) and could have substantially expanded the spatial impact of the low-oxygen equatorial Atlantic. Second, Cretaceous oceanic anoxic events (OAEs; Jenkyns, 2010), which are global-scale climate/carbon cycle perturbations, are predicted to have the most substantial impact in terms of deoxygenation and carbon burial on the restricted tropical Atlantic (Monteiro et al., 2012) (Figure **F9**). For OAE-2 (Cenomanian/Turonian boundary ocean anoxic event), thought to be triggered by the eruption of the Caribbean igneous province (du Vivier et al., 2015), drilling on the Pernambuco Plateau will allow distinctly mafic geochemical signatures (e.g., from chromium isotopes; Holmden et al., 2016) found north of the EAG to be traced into the South Atlantic basins. This would confirm that the source of these distinct mafic signatures is Caribbean volcanism and provide a water mass tracer to constrain exchange through the EAG. Third, sites on the Pernambuco Plateau will constrain the impact of hydroclimates on the redox and nutrient status of the tropical ocean as well as the rate and character of marine organic matter deposition. The intensity of precipitation associated with the Intertropical Convergence Zone (ITCZ) is a major control on the deposition of organic carbon in the deep Ivorian basin (Beckmann et al., 2005; Wagner et al., 2013) and the northern equatorial Atlantic (e.g., Kuypers et al., 2002). During supergreenhouse climates, such as the Cenomanian–Turonian, large-scale variations in Hadley cell circulation, weathering, and nutrient fluxes may have altered organic matter and nutrient cycling across a wide latitudinal band (Wagner et al., 2013). Lying at the southern extent of modern ITCZ variability, the proposed drill sites are located to test the latitudinal extent of orbital-controlled organic carbon burial and Hadley cell dynamics in supergreenhouse climates.

3. *Long-term paleoceanography of the Equatorial Atlantic Gateway*

How did opening of the EAG contribute to the evolution of global ocean circulation?

Known Cretaceous OAE black shale successions are spatially clustered in the tropics and subtropics of the Atlantic and Tethys Oceans and temporally clustered from the Aptian to the Santonian (Jenkyns, 2010). The absence of such widespread black shale events in the Cenozoic indicates a gradual system change into a state that was not susceptible to such pervasive deoxygenation. This change could reflect global cooling from the mid-Cretaceous supergreenhouse (Wilson and Norris, 2001) associated with the increased oxygenation (Weiss, 1970) and overturning rate of deep water masses. A complementary mechanism invokes enhanced deep-water circulation and ventilation driven by the progressive widening of the EAG (Friedrich and Erbacher, 2006; Handoh et al., 1999). This change in oceanic boundary conditions would help to explain the absence of black shale deposition in the Atlantic through early Paleogene transient warming events such as the Paleocene-Eocene Thermal Maximum (PETM) and, on longer-timescales, the early Eocene Climatic Optimum (EECO).

This ocean gateway hypothesis is supported by the progressive shift through the Campanian–Maastrichtian from siliciclastic, organic-rich deposits to high-carbonate pelagic oozes at sites on the western equatorial Atlantic margin (Friedrich and Erbacher, 2006). In the eastern equatorial Atlantic, the shift from black shales to carbonates is delayed until the early Paleogene but still has a one-way trend from organic carbon-rich to carbonate-rich systems, consistent with increased ventilation (Wagner, 2002). Some ~15 My later than the change in dominant sediment type at Demerara Rise is a marked convergence in equatorial and South Atlantic bottom water ε_{Nd} values into the range of Northern and Southern Component waters (Voigt et al., 2013), suggesting establishment of cross-equatorial circulation similar to the present day. The proposed deep-water sites are almost equidistant between Demerara Rise and Walvis Ridge and so are perfectly located to constrain the timing of this homogenization of bottom water ε_{Nd} signals in the South Atlantic. Together with the primary sites in intermediate water depths on the plateau, the deep-water sites will be invaluable in determining the links between the evolution of the EAG, deep-water circulation, and the long-term sensitivity of the global earth system to major climate and biogeochemical perturbations. These depth-distributed sites will also test the hypothesis that a stratified water mass helped "trap" nutrients in deep waters, stimulating oxygen drawdown and organic matter burial (Jiménez Berrocoso et al., 2010). New Re-Os data have the potential to establish an Os-isotope record of Atlantic seawater south of the EAG. The short oceanic residence time of Os (~10–50 ky) allows the composition of highly restricted basins to evolve away from the mixed global seawater signal. Convergence of equatorial South Atlantic seawater Os-isotope compositions with the global trend would be an additional constraint on the rate of water mass exchange through the EAG.

Long-term records of Atlantic deep-water chemistry and carbonate compensation depth

With primary sites at both intermediate water depths (Sites PER-9B, PER-12B, and PER-13A) and deep-water locations (Site PER-4A) just above the modern carbonate compensation depth (CCD), Expedition 388 will aim, for the first time, to constrain the evolution of the equatorial Atlantic CCD throughout the latest Cretaceous and Cenozoic. New depth- and latitudinal-transect ocean drilling has provided CCD reconstructions for the last ~50 My with unprecedented detail in the equatorial Pacific (Pälike et al., 2012). These reconstructions clearly show the impact of long-term climate evolution on ocean carbonate chemistry, most notably the transition to more saturated deep waters in the late Cenozoic icehouse climate state. Constraining the wider whole ocean carbonate system, however, requires improved records from the truly deep ocean (deeper than 4 km) over both secular timescales and during short-term climate perturbations (Greene et al., in press). This is especially the case in the Atlantic where, for the early Paleogene and likely the Late Cretaceous, there are no >4 km water depth records of carbonate deposition from the South, equatorial, or tropical North Atlantic (Greene et al., in press). In particular, proposed climate-weathering feedbacks for the recovery from transients, such as the early Paleogene hypethermal events, predict distinct patterns of carbonate (and silica) burial "overshoots" that should be detectable in the proposed deep-water locations (Penman et al., 2016). Calcium carbonate contents in regional core-top databases indicate $CaCO_3$ contents of ~50 wt% in the deep water off plateau locations in recent near-surface sediments (Figure **F10**).

4. *Limits of tropical climates and ecosystems under conditions of extreme warmth*

Do negative feedbacks limit tropical temperatures in greenhouse climate states?

There are strong indications that patterns of greenhouse gas–forced global warming are nonuniform with latitude and have exaggerated temperature increases at higher latitudes (Masson-Delmotte et al., 2013). Paleotemperature reconstructions from ancient greenhouse intervals of Earth history strongly support these patterns in excess of ice albedo and elevation feedbacks (Lunt et al., 2012). Long-term records of tropical sea-surface temperatures show relatively little change through multimillion-year intervals of pronounced global temperature change, such as early to late Eocene cooling (Pearson et al., 2007) or Turonian (mid-Cretaceous) (MacLeod et al., 2013), although there is evidence for pronounced tropical warming across the major early Paleogene hyperthermal events such as the PETM (Aze et al., 2014; Stap et al., 2010). If correct, the response to transient events suggests only a weak tropical thermostat in response to greenhouse gas forcing, whereas the longer term trends may reflect the partial offsetting of greenhouse gas forcing by progressive paleogeographic change, although there is little evidence for this from modeling studies (Lunt et al., 2016). The biggest uncertainty and limitation in answering these questions is the quality, quantity, and geographic spread of existing tropical sea-surface temperature estimates from greenhouse climate intervals (Dunkley Jones et al., 2013; Lunt et al., 2012).

Expedition 388 aims to recover lower Cenozoic biomarker and microfossil records from relatively shallow paleowater depths (~1500 m; Sites PER-9B, PER-12B, and PER-13A) in potentially clay-rich, outer continental margin successions to provide the necessary substrates for proxy analyses to address this key component of global climate evolution. Clay-rich sediments raise the preservation potential of both molecular fossils (biomarkers) and carbonate microfossils by slowing the rate of postburial oxic diagenesis of organic matter that is typical of low accumulation–rate marine sediments and by slowing the rate of diagenetic recrystallization that is characteristic of carbonate-rich pelagic oozes (Pearson et al., 2001; Sexton et al., 2006). The recovery of biomarkers and well-preserved carbonates also allows deployment of multiproxy approaches that significantly reduce the uncertainty inherent with any single-proxy methodology. These relatively proximal environments are also likely to contain terrestrial-derived material including pollen and spore records as well as biomarkers suitable for quantifying terrestrial paleotemperature and terrestrial carbon cycling. Such proxy records will be able to quantify the maximum warming of sea-surface and terrestrial temperatures during peak greenhouse climate states, especially the EECO and the PETM, which are both key targets for new paleoclimate modeling efforts. This data-model approach will address the magnitude and nature of any tropical thermostat mechanism that limits low-latitude warming with extreme greenhouse gas forcing.

Are tropical ecosystems resilient to extreme warmth, and what are the combined impacts of temperature and low-oxygen conditions on marine ecosystem functioning?

Low-latitude environments and climates are typically viewed as stable over long time periods (Greenwood and Wing, 1995; Norris et al., 2013; Pearson et al., 2007), resulting in the development of complex ecosystems with high biodiversity (e.g., Jablonski et al., 2006). Yet, under conditions of rapid warming, such as that predicted for the twenty-first century, tropical ecosystems may be among the most sensitive environments to adverse change because taxa are living at or close to their environmental and/or physiological limits (Tittensor et al., 2010).

It is thus a fundamental question whether there are processes and thresholds in the physical climate systems that pose limits to life or that may decouple the relationship between temperature and biodiversity seen in the present day. In early Paleogene conditions of peak warmth, climate model simulations predict extreme tropical continental surface air temperature (Huber and Caballero, 2011; Lunt et al., 2012) that approaches the thresholds for tropical plant heat death (Huber, 2008), coral reef survival (Scheibner and Speijer, 2008), and bleaching of symbiont-hosting foraminifers (Edgar et al., 2013). These climate models are also seemingly at odds with floristic records of peak diversities in the neotropics during the early Cenozoic (Jaramillo et al., 2006). Recovery of sediments from the restricted Cretaceous equatorial South Atlantic would also determine the combined impacts of extreme seawater chemistry, low oxygen, and climatic warmth on marine biota over a range of conditions and timescales. These sediment records would address the rates of species/community loss, recovery, and long-term restructuring associated with deoxygenation and hyperthermy. Furthermore, they would also address the role of bacterial nitrogen fixers in sustaining high rates of productivity as well as the more general composition of algal, bacterial, and archaeal communities in response to local oxygenation, temperature, and nutrient conditions. To properly understand the controls on tropical ecosystems during intervals of extreme warming requires both reliable paleotemperature estimation and microfossil and biomarker records of marine and terrestrial ecosystem composition and function.

The Brazilian margin represents a unique drilling opportunity because it has consistently been within a narrow latitudinal window in the tropical South Atlantic for the past ~100 My. Therefore, highly resolved records of terrestrial and marine ecosystem compositions from a single region would enable us to set limits on the maximum rate and magnitude of environmental change to which organisms are able to adapt, to understand the biological mechanisms adopted by different organisms to cope with environmental stress (ecology versus evolution), and to disentangle the dominant controls on ecological change. Finally, drilling would be able to address the question of whether there are common (and therefore predictable) biotic signals associated with environmental change.

Operations plan/drilling strategy

Proposed drill sites

The Expedition 388 drilling and coring strategy is designed to maximize recovery of core material at four primary locations to meet the scientific objectives outlined above. Operations will be focused in two key areas: first, in deep water (~4500 m depth) just off the Pernambuco Plateau, targeting oceanic basement and the overlying sediment cover (primary Site PER-4A; alternate Sites PER-5A, PER-7A, and PER-11A), and second, a series of intermediate water depth sites (~2000 m depth) located in relatively thin sedimentary basins on the outer margins of the Pernambuco Plateau (primary Sites PER-9B, PER-12B, and PER-13A; alternate Sites PER-6B and PER-8A). With the port call in Recife, Brazil, within a few hours transit time of all primary and alternate sites, operations time is fully maximized to meet the science objectives of the expedition. We propose to use a combination of the advanced piston corer (APC), extended core barrel (XCB), and the rotary core barrel (RCB) systems to maximize core quality and recovery in the upper sections while reaching the deep-target horizons and recovering basaltic basement with dedicated RCB drilling at two primary sites (Sites PER-4A and PER-9B) (Tables **T1**, **T2**).

To minimize operations risk, drilling operations will commence with the deepest water (4452 m) and deepest penetration (999 m) primary site location Site PER-4A, which addresses the early post-rift science objectives of Objectives 1 and 2. Operations will commence with two APC/XCB holes to refusal (estimated ~600 m) with downhole logging in the second hole, followed by a bit change to RCB and installation of casing to 400 meters below seafloor (mbsf) (Table **T1**). RCB drilling and coring will continue from 400 mbsf to basement (~979 mbsf). At basement, coring will continue until suitable basaltic material has been recovered for the purposes of dating, to meet science Objective 1 above, to a maximum Environmental Protection and Safety Panel (EPSP)-approved depth of 1200 mbsf. At the end of hole, we will drop the bit, condition the hole, and log from the bottom of casing to total depth. Alternate sites (PER-5A, PER-7A, and PER-11A) in deep water follow a similar operations plan to Site PER-4A, except that with the deeper water and thicker sediment thickness of Site PER-11A, coring operations are limited to the uppermost 1000 m of sediment, ~400 m above basement.

Expedition 388 will target three primary sites in intermediate water depths on the Pernambuco Plateau (Sites PER-9B, PER-12B, and PER-13A) to address Objectives 3 and 4. At Site PER-9B, two APC/XCB holes will drill to and tag basement, estimated to be ~590 mbsf. These holes will be followed by a bit change and RCB drilling of a third hole with the aim of recovering the sediment–basement transition and at least 20 m of volcanic basement. The two other primary sites on the plateau, Sites PER-12B and PER-13A, will be triple cored with APC/XCB holes to maximum depths of 400 and 500 mbsf, respectively. There are two alternate sites on the plateau, Sites PER-6B and PER-8A. Site PER-6B has a thick sediment sequence (~1210 m) over basement with an operations plan of APC/XCB coring to refusal, followed by a bit change to RCB and drill-in casing ~650 m and coring to and into basement (~1230 m). Site PER-8A operations plan is for triple APC/XCB coring to a maximum depth of 400 mbsf.

Logging/downhole measurements strategy

Downhole wireline logging

Wireline logging is planned for all sites, with logging in both Holes B (APC/XCB) and C (RCB) for deep-penetration location Site PER-4A. We will use the triple combination (triple combo) tool string, which logs formation resistivity, density, porosity, natural (spectral) gamma radiation, magnetic susceptibility, and borehole diameter. The Formation MicroScanner (FMS)-sonic tool string will provide an oriented 360° resistivity image of the borehole wall and logs of formation acoustic velocity, natural gamma radiation, and borehole diameter. Downhole log data provide the only in situ formation characterization and are the only data where core recovery is incomplete, allowing interpretations even in core gaps. For example, individual clasts will be apparent in FMS resistivity images, and silica-cemented layers will be clear in the resistivity and density logs. Porosity, gamma ray, sonic, and density logs together will provide additional constraints on the depositional history. A check shot survey with the Versatile Seismic Imager (VSI) is also planned for all site locations to allow depth-to-traveltime conversion. A combination of sonic velocity and density data will be used to generate a synthetic seismic profile at each site, hence enabling lithostratigraphy to be tied to seismic stratigraphy and thus extension of the knowledge gained from the cores over a much broader area.

For more information on the downhole logging tools, see **http://iodp.tamu.edu/tools/logging**.

Downhole tools

Temperature formation measurements will be conducted using the third-generation advanced piston corer temperature tool (APCT-3). This tool is housed in an APC cutting shoe and is deployed with the APC core barrel. The APCT-3 is only used in soft sediments.

Core orientation will be measured on all APC cores using the Icefield MI-5 multishot core orientation tool. The MI-5 tool collects azimuth, inclination, toolface gravity, toolface magnetism, total magnetic field strength, magnetic dip angle, and probe temperature.

Risks and contingency

We expect to encounter minimal operational risks during Expedition 388. The proposed operations plan includes 2 days of contingency time in case of any delays in drilling, coring, or logging operations (Table **T1**). If operations need to be cut because of time constraints, the overall expedition schedule is structured in order of site priority. Operational decisions for time allocation will be based on an assessment of the recovered stratigraphy and the ability to meet the primary science objectives. Options to reduce operations time include reducing downhole logging activities, reducing from three to two holes at primary sites on the plateau (Sites PER-9B, PER-12B, and PER-13A), and withdrawing operations at Site PER-13A.

Operational risks

The proposed penetration at Site PER-4A (999 m) may prove challenging for successful collecting of cores and log data. Hole stability is always a risk during coring and logging operations, and the risk increases with longer open-hole sections. Casing long open-hole sections (especially over intervals of unconsolidated sediment) is the best way to mitigate this risk and ensure that deep objectives can be achieved. In our plan, Site PER-4A will be cased to ~400 mbsf to retrieve deeper sediment and basement samples. A stuck drill string (or logging tool string) is always a risk during operations and can consume expedition time with attempts to extract the stuck drill string. If the drill string cannot be extracted, then additional time is spent to sever the stuck pipe. This process can result in complete loss of the hole, lost equipment, and lost time while starting a new hole. *JOIDES Resolution* generally carries sufficient spare drilling equipment to enable continuation of coring, but the time lost to the expedition can be significant. The sites may contain shallow gas, which can lead to core expansion and, in extreme cases, exploding core liners. Core expansion has a detrimental effect on sediment quality and contributes to core disturbance. The Expedition 388 sites are located near active petroleum lease blocks and, although they have been assessed by the IODP EPSP, there is still a small possibility that hydrocarbons may be encountered. The JRSO has onboard safety monitoring procedures to measure gas contents and concentrations of sediment cores and if necessary abandon the hole.

Downhole logging risks

The upper parts of holes have been open longer before logging, and high levels of fluid circulation might have been used to raise the cuttings and clear the hole. Therefore, the hole could be washed out (wide) over intervals through unconsolidated sediment, which reduces log quality for those tools that need good contact with the borehole wall (e.g., density, porosity, FMS resistivity images, and VSI check shots). There is also a risk of bridging, where the hole closes up, which would mean either not reaching the total depth of the hole or, in the worst-case scenario, getting a tool string stuck in the hole. We will obtain hole condition information needed to plan for logging while coring and during the preparations for downhole logging. Sufficient heavy mud will be available to displace each hole for logging to reduce the risk of hole collapse during wireline logging. Permitting is required to operate the VSI tool.

Sampling and data sharing strategy

Shipboard and shore-based researchers should refer to the IODP Sample, Data, and Obligations Policy and Implementation Guidelines posted on the Web at **http://www.iodp.org/top-resources/program-documents/policies-and-guidelines**. This document outlines the policy for distributing IODP samples and data to research scientists, curators, and educators. The document also defines the obligations that sample and data recipients incur. The Sample Allocation Committee (SAC; composed of Co-Chief Scientists, Staff Scientist, and IODP Curator on shore and curatorial representative on board ship) will work with the entire science party to formulate a formal expedition-specific sampling plan for shipboard and postcruise sampling.

Shipboard scientists are expected to submit sample requests (at **http://iodp.tamu.edu/curation/samples.html**) 4 months before the beginning of the expedition. Based on sample requests (shore based and shipboard) submitted by this deadline, the SAC will prepare a tentative sampling plan, which will be revised on the ship as dictated by recovery and cruise objectives. The sampling plan will be subject to modification depending upon the actual material recovered and collaborations that may evolve between scientists during the expedition. Modification of the strategy during the expedition must be approved by the Co-Chief Scientists, Staff Scientist, and curatorial representative on board ship.

The minimum permanent archive will be the standard archive half of each core. All sample frequencies and sizes must be justified on a scientific basis and will depend on core recovery, the full spectrum of other requests, and the cruise objectives. Some redundancy of measurement is unavoidable, but minimizing the duplication of measurements among the shipboard party and identified shore-based collaborators will be a factor in evaluating sample requests.

If some critical intervals are recovered, there may be considerable demand for samples from a limited amount of cored material. These intervals may require special handling, a higher sampling density, reduced sample size, or continuous core sampling by a single investigator. A sampling plan coordinated by the SAC may be required before critical intervals are sampled.

Our plan is to restrict shipboard sampling to those samples required for shipboard characterization/measurements, any samples that are ephemeral, and possibly very limited, very low resolution samples for personal research that are required to define plans for the postcruise sampling meeting. Whole-round samples may be taken for, but not limited to, interstitial water measurements and petrophysical measurements as dictated by the primary cruise objectives, approved research plans, and the shipboard sampling plan that must be finalized during the first few days of the expedition. Nearly all personal sampling for postexpedition research will be postponed until a shore-based sampling meeting that will be implemented ~3–5 months after the end of Expedition 388 at the IODP Bremen Core Repository (Bremen, Germany). All collected data and samples will be protected by a 1 y moratorium period following the completion of the postexpedition sampling meeting, during which time data and samples will be available only to the Expedition 388 science party.

Expedition scientists and scientific participants

The current list of participants for Expedition 388 can be found at **http://iodp.tamu.edu/scienceops/expeditions/equatorial_atlantic_gateway.html**.

References

Arai, M., 2014. Aptian/Albian (Early Cretaceous) paleogeography of the South Atlantic: a paleontological perspective. *Brazilian Journal of Geology,* 44(2):339–350. **http://www.scielo.br/scielo.php?script=sci_arttext&pid=S2317-48892014000100339**

Arai, M., and Botelho Neto, J., 1996. Biostratigraphy of the marine Cretaceous of the southern and southeastern Brazilian marginal basins, based on dinoflagellates. *SAMC (South Atlantic Mesozoic Correlations) News,* 6:15–16.

Archer, D.E., 1996. An atlas of the distribution of calcium carbonate in sediments of the deep sea. *Global Biogeochemical Cycles,* 10(1):159–174. **https://doi.org/10.1029/95GB03016**

Aze, T., Pearson, P.N., Dickson, A.J., Badger, M.P.S., Bown, P.R., Pancost, R.D., et al., 2014. Extreme warming of tropical waters during the Paleocene–Eocene Thermal Maximum. *Geology,* 42(9):739–742. **https://doi.org/10.1130/G35637.1**

Beckmann, B., Flögel, S., Hofmann, P., Schulz, M., and Wagner, T., 2005. Orbital forcing of Cretaceous river discharge in tropical Africa and ocean response. *Nature,* 437(7056):241–244. **https://doi.org/10.1038/nature03976**

Blaich, O.A., Tsikalas, F., and Faleide, J.I., 2008. Northeastern Brazilian margin: regional tectonic evolution based on integrated analysis of seismic reflection and potential field data and modelling. *Tectonophysics,* 458(1–4):51–67. **https://doi.org/10.1016/j.tecto.2008.02.011**

Buarque, B.V., Barbosa, J.A., Magalhães, J.R.G., Cruz Oliveira, J.T., and Correia Filho, O.J., 2016. Post-rift volcanic structures of the Pernambuco Plateau, northeastern Brazil. *Journal of South American Earth Sciences,* 70:251–267. **https://doi.org/10.1016/j.jsames.2016.05.014**

Caixeta, J.M., Ferreira, T.S., Machado, D.L., Jr., Teixeira, J.L., and Romeiro, M.A.T., 2014. Albian Rift Systems in the Northeastern Brazilian Margin: an example of rifting in hyper-extended continental crust. *AAPG Search and Discovery,* 30378. **http://www.searchanddiscovery.com/documents/2014/30378caixeta/ndx_caixeta.pdf**

Crosby, A.G., McKenzie, D., and Sclater, J.G., 2006. The relationship between depth, age and gravity in the oceans. *Geophysical Journal International,* 166(2):553–573. **https://doi.org/10.1111/j.1365-246X.2006.03015.x**

Darros de Matos, R.M., 1999. History of the northeast Brazilian rift system: kinematic implications for the break-up between Brazil and West Africa. *In* Cameron, N.R., Bate, R.H., and Clure, V.S. (Eds.), *The Oil and Gas Habitats of the South Atlantic.* Geological Society Special Publication, 153:55–73. **https://doi.org/10.1144/GSL.SP.1999.153.01.04**

Davison, I., 2007. Geology and tectonics of the South Atlantic Brazilian salt basins. *In* Ries, A.C., Butler, R.W.H., and Graham, R.H. (Eds.), *Deformation of the Continental Crust: The Legacy of Mike Coward.* Geological Society Special Publication, 272:345–359. **https://doi.org/10.1144/GSL.SP.2007.272.01.18**

Du Vivier, A.D.C., Selby, D., Condon, D.J., Takashima, R., and Nishi, H., 2015. Pacific $^{187}Os/^{188}Os$ isotope chemistry and U–Pb geochronology: synchroneity of global Os isotope change across OAE 2. *Earth and Planetary Science Letters,* 428:204–216. **https://doi.org/10.1016/j.epsl.2015.07.020**

Dunkley Jones, T., Lunt, D.J., Schmidt, D.N., Ridgewell, A., Sluijs, A., Valdes, P.J., and Maslin, M., 2013. Climate model and proxy data constraints on ocean warming across the Paleocene–Eocene Thermal Maximum. *Earth-Science Reviews,* 125:123–145. **https://doi.org/10.1016/j.earscirev.2013.07.004**

Edgar, K.M., Bohaty, S.M., Gibbs, S.J., Sexton, P.F., Norris, R.D., and Wilson, P.A., 2012. Symbiont "bleaching" in planktic foraminifera during the Middle Eocene Climatic Optimum. *Geology,* 41(1):15–18. **https://doi.org/10.1130/G33388.1**

Falkowski, P.G., 1997. Evolution of the nitrogen cycle and its influence on the biological sequestration of CO_2 in the ocean. *Nature,* 387(6630):272–275. **https://doi.org/10.1038/387272a0**

Friedrich, O., and Erbacher, J., 2006. Benthic foraminiferal assemblages from Demerara Rise (ODP Leg 207, western tropical Atlantic): possible evidence for a progressive opening of the equatorial Atlantic gateway. *Cretaceous Research,* 27(3):377–397. **https://doi.org/10.1016/j.cretres.2005.07.006**

Friedrich, O., Norris, R.D., and Erbacher, J., 2012. Evolution of middle to Late Cretaceous oceans—a 55 m.y. record of Earth's temperature and carbon cycle. *Geology,* 40(2):107–110. **https://doi.org/10.1130/G32701.1**

Granot, R., and Dyment, J., 2015. The Cretaceous opening of the South Atlantic Ocean. *Earth and Planetary Science Letters,* 414:156–163. **https://doi.org/10.1016/j.epsl.2015.01.015**

Granot, R., Dyment, J., and Gallet, Y., 2012. Geomagnetic field variability during the Cretaceous Normal Superchron. *Nature Geoscience,* 5(3):220–223. **https://doi.org/10.1038/ngeo1404**

Greene, S.E., Ridgwell, A., Kirtland Turner, S., Schmidt, D.N., Pälike, H., Thomas, E., Greene, L.K., and Hoogakker, B.A.A., in press. Early Cenozoic decoupling of climate and carbonate compensation depth trends. *Paleoceanography and Paleoclimatology.* **https://doi.org/10.1029/2019PA003601**

Greenwood, D.R., and Wing, S.L., 1995. Eocene continental climates and latitudinal temperature gradients. *Geology,* 23(11):1044–1048. **https://doi.org/10.1130/0091-7613(1995)023<1044:ECCALT>2.3.CO;2**

Handoh, I.C., Bigg, G.R., Jones, E.J.W., and Inoue, M., 1999. An ocean modeling study of the Cenomanian Atlantic: equatorial paleo-upwelling, organic-rich sediments and the consequences for a connection between the proto-North and South Atlantic. *Geophysical Research Letters,* 26:223–226. **https://doi.org/10.1029/1998GL900265**

Heine, C., and Brune, S., 2014. Oblique rifting of the equatorial Atlantic: why there is no Saharan Atlantic Ocean. *Geology,* 42(3):211–214. **https://doi.org/10.1130/G35082.1**

Heine, C., Zoethout, J., and Müller, R.D., 2013. Kinematics of the South Atlantic rift. *Solid Earth,* 4(2):215–253. **https://doi.org/10.5194/se-4-215-2013**

Holmden, C., Jacobson, A.D., Sageman, B.B., and Hurtgen, M.T., 2016. Response of the Cr isotope proxy to Cretaceous Ocean Anoxic Event 2 in a pelagic carbonate succession from the Western Interior Seaway. *Geochimica et Cosmochimica Acta,* 186:277–295. **https://doi.org/10.1016/j.gca.2016.04.039**

Huber, M., 2008. A hotter greenhouse? *Science,* 321(5887):353–354. **https://doi.org/10.1126/science.1161170**

Huber, M., and Caballero, R., 2011. The early Eocene equable climate problem revisited. *Climate of the Past,* 7(2):603–633. **https://doi.org/10.5194/cp-7-603-2011**

Jablonski, D., Roy, K., and Valentine, J.W., 2006. Out of the tropics: evolutionary dynamics of the latitudinal diversity gradient. *Science,* 314(5796):102–106. **https://doi.org/10.1126/science.1130880**

Jaramillo, C., Rueda, M.J., and Mora, G., 2006. Cenozoic plant diversity in the Neotropics. *Science,* 311(5769):1893–1896. **https://doi.org/10.1126/science.1121380**

Jenkyns, H.C., 2010. Geochemistry of oceanic anoxic events. *Geochemistry, Geophysics, Geosystems,* 11(3):Q03004. **https://doi.org/10.1029/2009GC002788**

Jiménez Berrocoso, Á., MacLeod, K.G., Huber, B.T., Lees, J.A., Wendler, I., Bown, P.R., Mweneinda, A.K., Isaza Londoño, C., and Singano, J.M., 2010. Lithostratigraphy, biostratigraphy and chemostratigraphy of Upper Cretaceous sediments from southern Tanzania: Tanzania Drilling Project Sites 21–26. *Journal of African Earth Sciences,* 57(1–2):47–69. **https://doi.org/10.1016/j.jafrearsci.2009.07.010**

Keeling, R.F., Körtzinger, A., and Gruber, N., 2010. Ocean deoxygenation in a warming world. *Annual Review of Marine Science,* 2(1):199–229. **https://doi.org/10.1146/annurev.marine.010908.163855**

Koutsoukos, E.A.M., 1992. Late Aptian to Maastrichtian foraminiferal biogeography and paleoceanography of the Sergipe Basin, Brazil. *Palaeogeography, Palaeoclimatology, Palaeoecology,* 92(3–4):295–324. **https://doi.org/10.1016/0031-0182(92)90089-N**

Koutsoukos, E.A.M., Leary, P.N., and Hart, M.B., 1989. *Favusella* Michael (1972): evidence of ecophenotypic adaptation of a planktonic foraminifer to shallow-water carbonate environments during the mid-Cretaceous. *Journal of Foraminiferal Research,* 19(4):324–336. **https://doi.org/10.2113/gsjfr.19.4.324**

Kuypers, M.M.M., Pancost, R.D., Nijenhuis, I.A., and Sinninghe Damsté, J.S., 2002. Enhanced productivity led to increased organic carbon burial in the euxinic North Atlantic Basin during the late Cenomanian oceanic anoxic event. *Paleoceanography,* 17(4):1051. **https://doi.org/10.1029/2000PA000569**

Lunt, D.J., Dunkley Jones, T., Heinemann, M., Huber, M., LeGrande, A., Winguth, A., Loptson, C., Marotzke, J., Roberts, C.D., Tindall, J., Valdes, P., et al., 2012. A model-data comparison for a multi-model ensemble of early Eocene atmosphere-ocean simulations: EoMIP. *Climate of the Past,* 8(2):1716–1736. **https://doi.org/10.5194/cpd-8-1229-2012**

Lunt, D.J., Farnsworth, A., Lopston, C., Foster, G.L., Markwick, P., O'Brien, C.L., Pancost, R.D., Robinson, S.A., and Wrobel, N., 2016. Palaeogeographic controls on climate and proxy interpretation. *Climate of the Past,* 12(5):1181–1198. **https://doi.org/10.5194/cp-12-1181-2016**

Lyons, T.W., Reinhard, C.T., and Planavsky, N.J., 2014. Evolution: a fixed-nitrogen fix in the early ocean? *Current Biology,* 24(7):R276–R278. **https://doi.org/10.1016/j.cub.2014.02.034**

MacLeod, K.G., Huber, B.T., Jiménez Berrocoso, Á., and Wendler, I., 2013. A stable and hot Turonian without glacial $\delta^{18}O$ excursions is indicated by exquisitely preserved Tanzanian foraminifera. *Geology,* 41(10):1083–1086. **https://doi.org/10.1130/G34510.1**

MacLeod, K.G., Londoño, C.I., Martin, E.E., Jiménez Berrocoso, Á., and Basak, C., 2011. Changes in North Atlantic circulation at the end of the Cretaceous greenhouse interval. *Nature Geoscience,* 4(11):779–782. **https://doi.org/10.1038/ngeo1284**

Magalhães, J., Barbosa, J.A., Oliveira, J.T.C., and de lima Filho, M.F. 2014. Characterization of the ocean–continent transition in the Paraíba Basin and Natal Platform Region, NE Brazil. *Revista Brasileira de Geofísica,* 32(3):481–496. **https://doi.org/10.22564/rbgf.v32i3.504**

Marques, F.O., Nogueira, F.C.C., Bezerra, F.H.R., and de Castro, D.L., 2014. The Araripe Basin in NE Brazil: an intracontinental graben inverted to a high-standing horst. *Tectonophysics,* 630:251–264. **https://doi.org/10.1016/j.tecto.2014.05.029**

Masson-Delmotte, V., Schulz, M., Abe-Ouchi, A., Beer, J., Ganopolski, A., González Rouco, J.F., Jansen, E., et al., 2013. Information from paleoclimate archives. *In* Stocker, T.F., Qin, D., Plattner, G.-K., Tignor, M., Allen, S.K., Boschung, J., Nauels, A., Xia, Y., Bex, V., and Midgley, P.M. (Eds.), *Climate Change 2013: The Physical Science Basis. Contribution of Working Group I to the Fifth Assessment Report of the Intergovernmental Panel on Climate Change:* Cambridge, United Kingdom (Cambridge University Press), 383–464. **http://www.climatechange2013.org/images/report/WG1AR5_Chapter05_FINAL.pdf**

Monteiro, F.M., Pancost, R.D., Ridgwell, A., and Donnadieu, Y., 2012. Nutrients as the dominant control on the spread of anoxia and euxinia across the Cenomanian–Turonian Oceanic Anoxic Event (OAE2): model-data comparison. *Paleoceanography and Paleoclimatology,* 27(4):PA4209. **https://doi.org/10.1029/2012PA002351**

Moulin, M., Aslanian, D., and Unternehr, P., 2010. A new starting point for the south and equatorial Atlantic Ocean. *Earth-Science Reviews,* 98(1–2):1–37. **https://doi.org/10.1016/j.earscirev.2009.08.001**

Müller, R.D., Seton, M., Zahirovic, S., Williams, S.E., Matthews, K.J., Wright, N.M., Shephard, G.E., et al., 2016. Ocean basin evolution and global-scale plate reorganization events since Pangea breakup. *Annual Review of Earth and Planetary Sciences,* 44(1):107–138. **https://doi.org/10.1146/annurev-earth-060115-012211**

Müller, R.D., Sdrolias, M., Gaina, C., and Roest, W.R., 2008. Age, spreading rates, and spreading asymmetry of the world's ocean crust. *Geochemistry, Geophysics, Geosystems,* 9(4):Q04006. **https://doi.org/10.1029/2007GC001743**

Norris, R.D., Kirtland Turner, S., Hull, P.M., and Ridgwell, A., 2013. Marine ecosystem responses to Cenozoic global change. *Science,* 341(6145):492–498. **https://doi.org/10.1126/science.1240543**

Owens, J.D., Reinhard, C.T., Rohrssen, M., Love, G.D., and Lyons, T.W., 2016. Empirical links between trace metal cycling and marine microbial ecology during a large perturbation to Earth's carbon cycle. *Earth and Planetary Science Letters,* 449:407–417. **https://doi.org/10.1016/j.epsl.2016.05.046**

Pälike, H., Lyle, M.W., Nishi, H., Raffi, I., Ridgwell, A., Gamage, K., Klaus, A., et al., 2012. A Cenozoic record of the equatorial Pacific carbonate compensation depth. *Nature,* 488(7413):609–614. **https://doi.org/10.1038/nature11360**

Pearson, P.N., Ditchfield, P.W., Singano, J., Harcourt-Brown, K.G., Nicholas, C.J., Olsson, R.K., Shackleton, N.J., and Hall, M.A., 2001. Warm tropical sea surface temperatures in the Late Cretaceous and Eocene epochs. *Nature,* 413(6855):481–487. **https://doi.org/10.1038/35097000**

Pearson, P.N., van Dongen, B.E., Nicholas, C.J., Pancost, R.D., Schouten, S., Singano, J.M., and Wade, B.S., 2006. Stable warm tropical climate through the Eocene epoch. *Geology,* 35(3):211–214. **https://doi.org/10.1130/G23175A.1**

Penman, D.E., Turner, S.K., Sexton, P.F., Norris, R.D., Dickson, A.J., Boulila, S., Ridgwell, A., Zeebe, R.E., Zachos, J.C., Cameron, A., Westerhold, T., and Röhl, U., 2016. An abyssal carbonate compensation depth overshoot in the aftermath of the Palaeocene–Eocene Thermal Maximum. *Nature Geoscience,* 9:575–580. **https://doi.org/10.1038/ngeo2757**

Pérez-Díaz, L., and Eagles, G., 2017a. A new high-resolution seafloor age grid for the South Atlantic. *Geochemistry, Geophysics, Geosystems,* 18(1):457–470. **https://doi.org/10.1002/2016GC006750**

Pérez-Díaz, L., and Eagles, G., 2017b. South Atlantic paleobathymetry since early Cretaceous. *Scientific Reports,* 7(1):11819. **https://doi.org/10.1038/s41598-017-11959-7**

Poropat, S.F., and Colin, J.-P., 2012. Early Cretaceous ostracod biostratigraphy of eastern Brazil and western Africa: an overview. *Gondwana Research,* 22(3–4):772–798. **https://doi.org/10.1016/j.gr.2012.06.002**

Regali, M.S.P., and Santos, P.R.S., 1999. Palinoestratigrafia e geocronologia dos sedimentos albo-aptianos das bacias de Sergipe e de Alagoas—Brasil [paper presented at Simpósio sobre o Cretáceo do Brasil, Serra Negra-São Paulo, Brasil, 29 August–2 September 1999].

Savchuk, O.P., and Wulff, F., 2009. Long-term modeling of large-scale nutrient cycles in the entire Baltic Sea. *Hydrobiologia,* 629(1):209–224. **https://doi.org/10.1007/s10750-009-9775-z**

Scheibner, C., and Speijer, R.P., 2008. Late Paleocene–early Eocene Tethyan carbonate platform evolution—a response to long- and short-term paleoclimatic change. *Earth-Science Reviews,* 90(3–4):71–102. **https://doi.org/10.1016/j.earscirev.2008.07.002**

Sexton, P.F., Wilson, P.A., and Norris, R.D., 2006. Testing the Cenozoic multisite composite $\delta^{18}O$ and $\delta^{13}C$ curves: new monospecific Eocene records from a single locality, Demerara Rise (Ocean Drilling Program Leg 207). *Paleoceanography and Paleoclimatology,* 21(2):PA2019. **https://doi.org/10.1029/2005PA001253**

Shipboard Scientific Party, 1984. Site 530: southeastern corner of the Angola Basin. *In* Hay, W.W., Sibuet, J.-C, et al., *Initial Reports of the Deep Sea Drilling Project,* 75: Washington, DC (U.S. Government Printing Office), 29–285. **https://doi.org/10.2973/dsdp.proc.75.102.1984**

Slomp, C.P., Mort, H.P., Jilbert, T., Reed, D.C., Gustafsson, B.G., and Wolthers, M., 2013. Coupled dynamics of iron and phosphorus in sediments of an oligotrophic coastal basin and the impact of anaerobic oxidation of methane. *PloS One,* 8(4):e62386. **https://doi.org/10.1371/journal.pone.0062386**

Stap, L., Lourens, L.J., Thomas, E., Sluijs, A., Bohaty, S., and Zachos, J.C., 2010. High-resolution deep-sea carbon and oxygen isotope records of Eocene Thermal Maximum 2 and H2. *Geology,* 38(7):607–610. **https://doi.org/10.1130/G30777.1**

Tedeschi, L.R., Jenkyns, H.C., Robinson, S.R., Sanjinés, A.E.S., Viviers, M.C., Quintaes, C.M.S.P., and Vazquez, J.C., 2017. New age constraints on Aptian evaporites and carbonates from the South Atlantic: implications for Oceanic Anoxic Event 1a. *Geology,* 45(6):543–546. **https://doi.org/10.1130/G38886.1**

The Shipboard Scientific Party, 1977. Site 356: São Paulo Plateau. *In* Supko, P.R., Perch-Nielsen, K., et al., *Initial Reports of the Deep Sea Drilling Project,* 39: Washington, DC (U.S. Government Printing Office), 141–230. **https://doi.org/10.2973/dsdp.proc.39.105.1977**

Tittensor, D.P., Mora, C., Jetz, W., Lotze, H.K., Ricard, D., Vanden Berghe, E., and Worm, B., 2010. Global patterns and predictors of marine biodiversity across taxa. *Nature,* 466(7310):1098–1101. **https://doi.org/10.1038/nature09329**

Torsvik, T.H., Rousse, S., Labails, C., and Smethurst, M.A., 2009. A new scheme for the opening of the South Atlantic Ocean and the dissection of an Aptian salt basin. *Geophysical Journal International,* 177(3):1315–1333. **https://doi.org/10.1111/j.1365-246X.2009.04137.x**

Trabucho-Alexandre, J., Hay, W.W., and de Boer, P.L., 2012. Phanerozoic environments of black shale deposition and the Wilson cycle. *Solid Earth,* 3(1):29–42. **https://doi.org/10.5194/se-3-29-2012**

Valença, L.M.M., Neumann, V.H., and Mabesoone, J.M., 2003. An overview on Callovian–Cenomanian intracratonic basins of northeast Brazil: onshore stratigraphic record of the opening of the southern Atlantic. *Geologica Acta,* 1(3):261–275. **https://doi.org/10.1344/105.000001614**

Voigt, S., Jung, C., Friedrich, O., Frank, M., Teschner, C., and Hoffmann, J., 2013. Tectonically restricted deep-ocean circulation at the end of the Cretaceous greenhouse. *Earth and Planetary Science Letters,* 369–370:169–177. **https://doi.org/10.1016/j.epsl.2013.03.019**

Wagner, T., 2002. Late Cretaceous to early Quaternary organic sedimentation in the eastern equatorial Atlantic. *Palaeogeography, Palaeoclimatology, Palaeoecology,* 179(1–2):113–147. **https://doi.org/10.1016/S0031-0182(01)00415-1**

Wagner, T., Hofmann, P., and Flögel, S., 2013. Marine black shale deposition and Hadley cell dynamics: a conceptual framework for the Cretaceous Atlantic Ocean. *Marine and Petroleum Geology,* 43:222–238. **https://doi.org/10.1016/j.marpetgeo.2013.02.005**

Weiss, R.F., 1970. The solubility of nitrogen, oxygen and argon in water and seawater. *Deep-Sea Research and Oceanographic Abstracts,* 17(4):721–735. **https://doi.org/10.1016/0011-7471(70)90037-9**

Wilson, P.A., and Norris, R.D., 2001. Warm tropical ocean surface and global anoxia during the mid-Cretaceous period. *Nature,* 412(6845):425–429. **https://doi.org/10.1038/35086553**

Zachos, J., Pagani, M., Sloan, L., Thomas, E., and Billups, K., 2001. Trends, rhythms, and aberrations in global climate 65 Ma to present. *Science,* 292(5517):686–693. **https://doi.org/10.1126/science.1059412**

Table T1. Operations and time estimates for primary sites, Expedition 388.

Site	Location (latitude, longitude)	Seafloor depth (m)	Operations	Transit (days)	Drilling and coring (days)	Logging (days)
Recife			Begin expedition 5.0	Port call days		
			Transit 97 nmi to PER-04A @ 10.5 kt	0.4		
PER-04A	9°18.9600' S	4441	Hole A - APC/XCB coring to refusal (~600 mbsf)		5.3	
EPSP approved	33°52.3680' W		Hole B - APC/XCB coring to refusal (~600 mbsf); logging with triple combo and FMS-sonic		4.9	1.1
to 1200 mbsf			Hole C - Reentry installation - drill-in 10.75" casing with HRT system		2.9	
			Hole C - RCB coring from 400 mbsf to 999 mbsf; logging with triple combo, FMS-sonic, and VSI		8.0	1.5
			Subtotal days on-site: 23.8			
			Transit 45 nmi to PER-09B @ 10.5 kt	0.2		
PER-09B	8°33.7620' S	2288	Hole A - APC/XCB coring to 590 mbsf		3.7	
EPSP approved	33°55.2660' W		Hole B - APC/XCB coring to 590 mbsf		3.6	
to 650 mbsf			Hole C - Drill ahead to 575 mbsf; RCB core to 650 mbsf; logging with triple combo, FMS-sonic, and VSI		2.9	1.4
			Subtotal days on-site: 11.6			
			Transit 8 nmi to PER-12B @ 1.5 kt	0.2		
PER-12B	8°33.6000' S	2047	Hole A - APC/XCB coring to 400 mbsf		2.5	
EPSP approved	33°58.4280' W		Hole B - APC/XCB coring to 400 mbsf		2.0	
to 400 mbsf			Hole C - APC/XCB coring to 400 mbsf; logging with triple combo, FMS-sonic, and VSI		2.3	1.1
			Subtotal days on-site: 7.9			
			Transit 7nmi to PER-13A @ 1.5 kt	0.2		
PER-13A	8°33.9240' S	2139	Hole A - APC/XCB coring to 500 mbsf		3.2	
EPSP approved	33°56.0940' W		Hole B - APC/XCB coring to 500 mbsf		2.6	
to 500 mbsf			Hole C - APC/XCB coring to 500 mbsf; logging with triple combo, FMS-sonic, and VSI		2.8	1.2
			Subtotal days on-site: 9.8			
			Transit 64 nmi to Recife @ 10.5 kt	0.3		
Recife			End Expedition	1.2	46.8	6.3

Port call:	5.0	Total operating days:	54.3
Subtotal on-site:	53.1	Total expedition:	59.3

Table T2. Alternate sites, Expedition 388.

Site	Location (latitude, longitude)	Seafloor depth (m)	Operations	Drilling and Coring (days)	Logging (days)
PER-05A	7°34.7940' S	4413	Hole A - APC/XCB coring to 600 mbsf	5.5	0.0
EPSP approved	33°34.6020' W		Hole B - Reentry installation - drill-in 10.75" casing with HRT system	3.6	0.0
to 1150 mbsf			Hole B - RCB coring to 947 mbsf; logging with triple combo, FMS-sonic, and VSI	7.0	2.0
			Subtotal days on-site: 18.1		
PER-06B	8°27.3138' S	1835	Hole A - APC/XCB coring to 800 mbsf	4.4	0.0
EPSP approved	33°59.1720' W		Hole B - Reentry installation - drill-in 10.75" casing with HRT system	3.1	0.0
to 1230 mbsf			Hole B - RCB coring to 1228 mbsf; logging with triple combo, FMS Sonic and VSI	6.7	1.9
			Subtotal days on-site: 16.2		
PER-07A	9°13.9020' S	4412	Hole A - APC/XCB coring to 400 mbsf	3.8	0.0
EPSP approved	33°48.8160' W		Hole B - Reentry installation - drill-in 10.75" casing with HRT system	2.9	0.0
to 1100 mbsf			Hole B - RCB coring to 1015 mbsf; logging with triple combo, FMS-sonic, and VSI	8.0	1.5
			Subtotal days on-site: 16.2		
PER-08A	8°33.7500' S	2003	Hole A - APC/XCB coring to 400 mbsf	2.6	0.0
EPSP approved	33°59.4240' W		Hole B - APC/XCB coring to 400 mbsf	2.0	0.0
to 400 mbsf			Hole C - APC/XCB coring to 400 mbsf; logging with triple combo, FMS-sonic, and VSI	2.2	1.1
			Subtotal days on-site: 7.9		
PER-11A	9°32.4780' S	4704	Hole A - APC/XCB coring to refusal (~800 mbsf); logging with triple combo and FMS-sonic	7.6	1.3
EPSP approved	33°23.0040' W		Hole B - Reentry installation - drill-in 10.75" casing with HRT system	3.7	0.0
to 1000 mbsf			Hole B - RCB coring to 1000 mbsf; logging with triple combo, FMS-sonic, and VSI	4.7	1.6
			Subtotal days on-site: 18.8		

Figure F1. South and equatorial Atlantic tectonic structure superimposed on satellite-derived free-air gravity field with magnetic picks (Granot and Dyment, 2015). Red lines are flowlines calculated on the basis of the new Granot and Dyment (2015) stage rotations. The red star indicates the location of the Pernambuco Plateau.

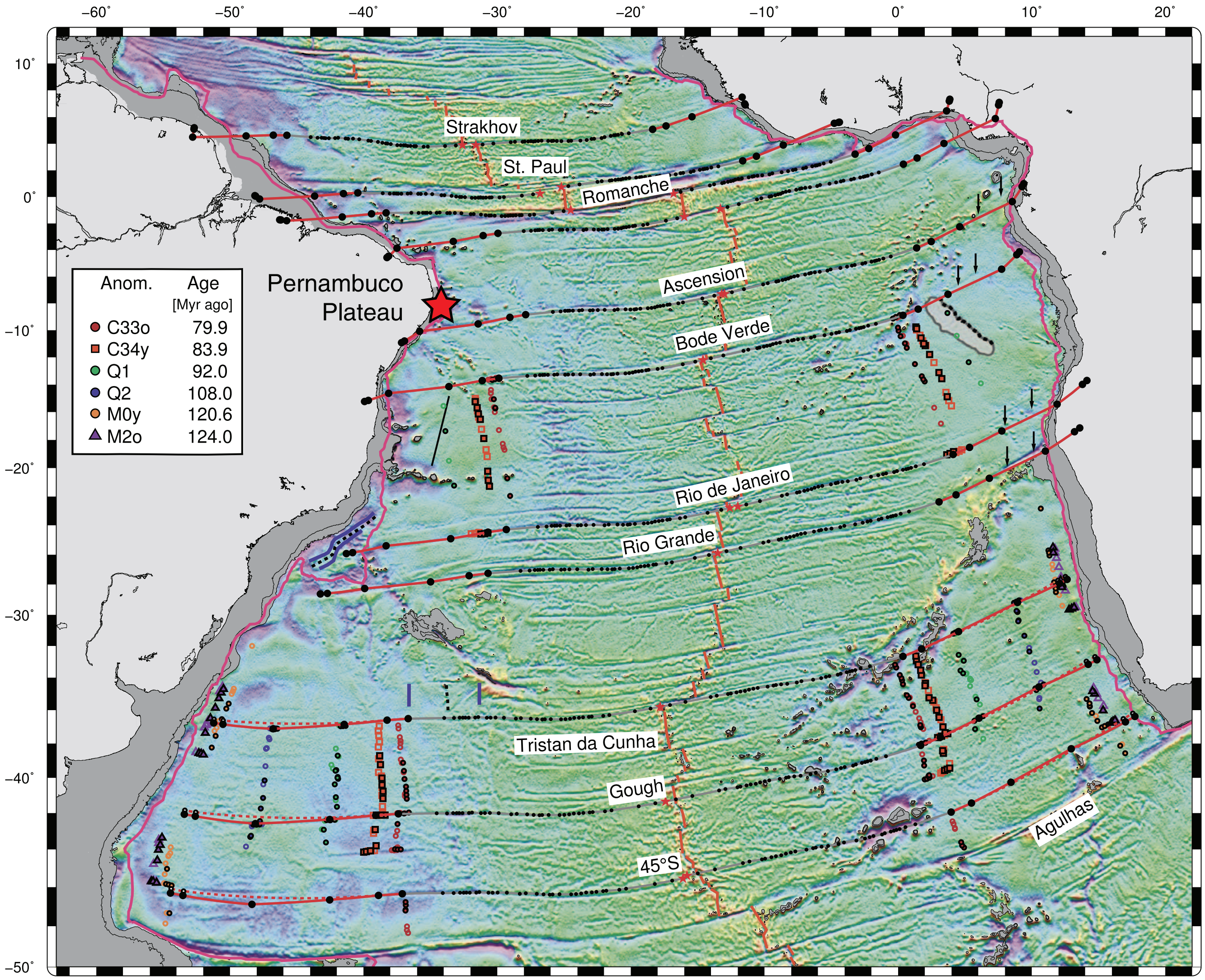

Figure F2. Borborema Province, northeast Brazil. Geological map over a digital elevation model, including sedimentary basins, basement rock ages, and the main shear zones and lineaments (Brazilian Geological Survey databank). Red dotted line = estimated position of continent–ocean boundary (COB) (after Blaich et al., 2008; Magalhães et al., 2014). S.Z. = sheer zone, Plataf. = platform, ND = north domain, TZ = Transversal Zone, SD = south domain.

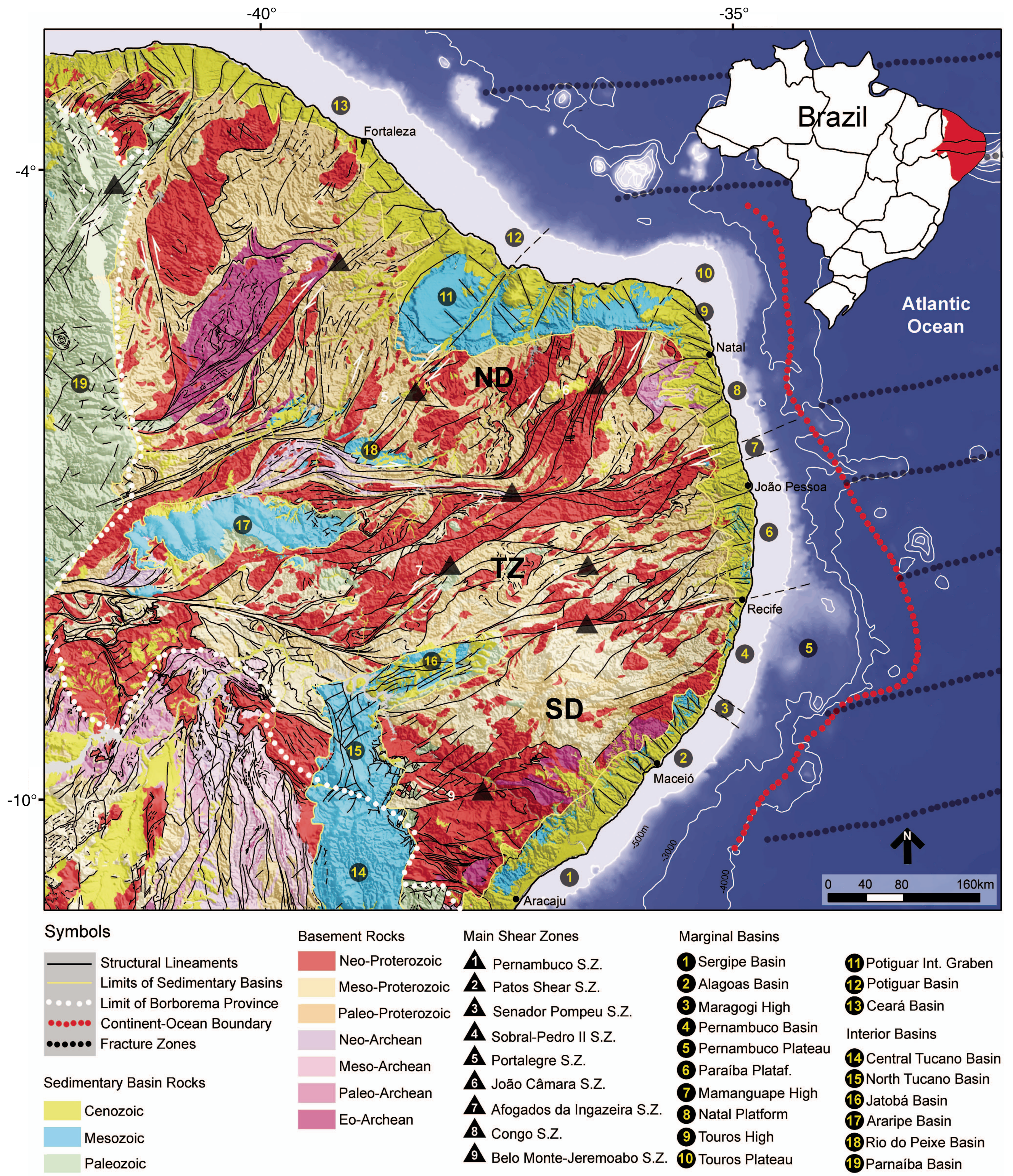

Figure F3. Tectonic reconstructions of the South and equatorial Atlantic domains (Heine et al., 2013). Red star = Pernambuco Plateau. A. 115 Ma just prior to complete rupture along the Walvis Ridge/Sao Paulo High and initiation(?) of deep-water connection to southern South Atlantic. (Continued on next page.)

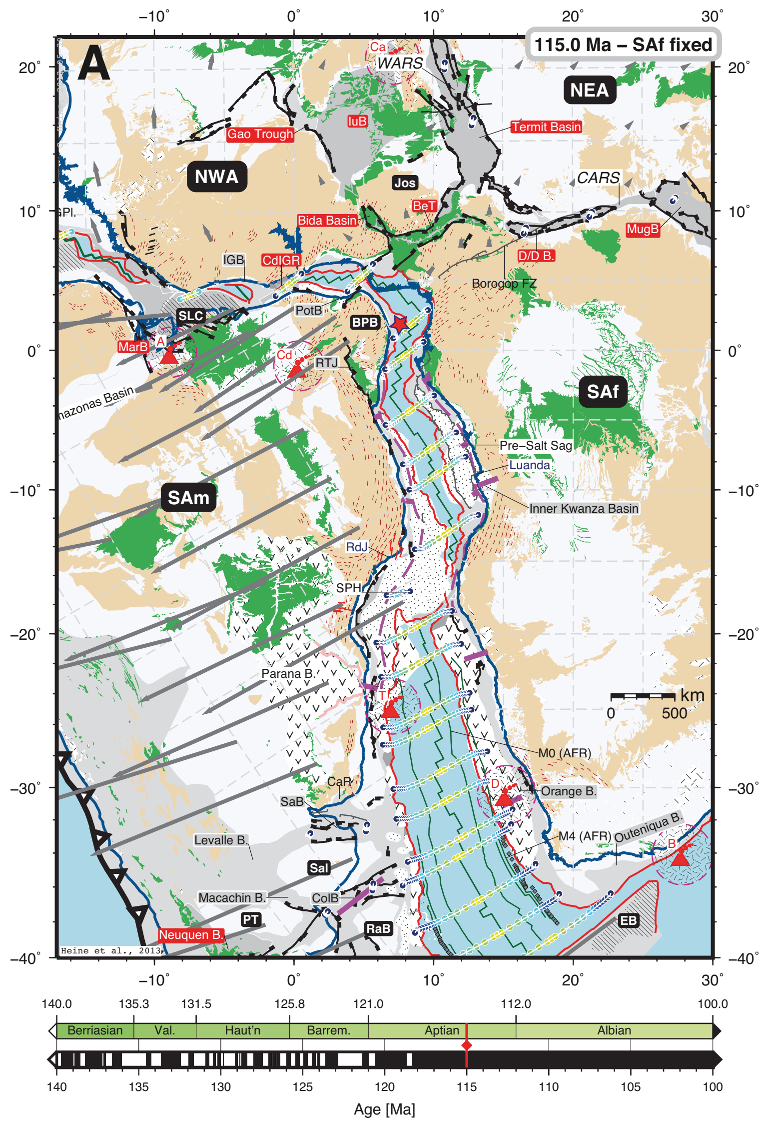

Figure F3 (continued). B. Equatorial Atlantic domain at 125 Ma and lithospheric breakup along the Sergipe-Alagoas/Rio Muni segment of the northern South Atlantic rift. C. 115 Ma, isolated oceanic basin segments open along equatorial Atlantic; mature seafloor spreading established between Africa and northeast Brazil. D. 105 Ma reconstruction shortly after final breakup between Africa and South America along the equatorial Atlantic rift system. NWA = Northwest Africa, NEA = Northeast Africa, SAm = South America, SAf = South Africa.

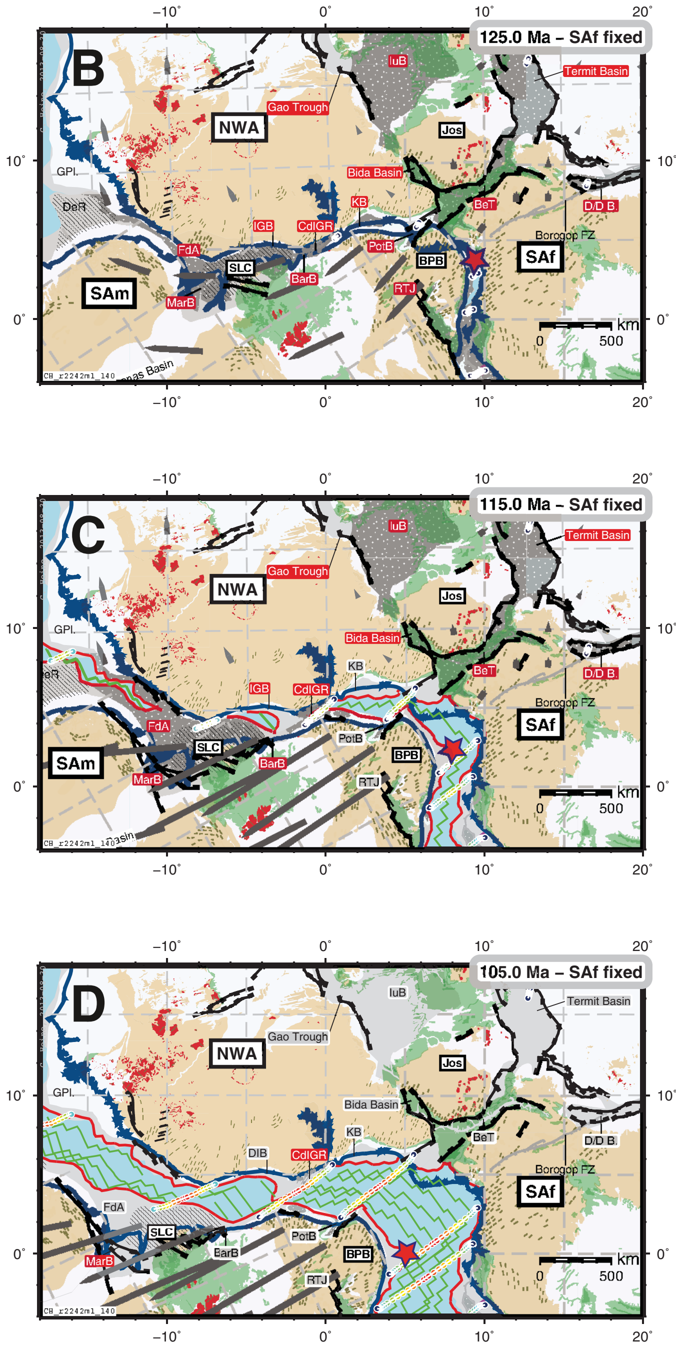

Figure F4. Existing DSDP/ODP/IODP drilling in the equatorial and South Atlantic; note very limited sampling of the Late Cretaceous (compiled by Alex Dickson; benthic $\delta^{18}O$ record is from Zachos et al. [2001] and Friedrich et al. [2012]).

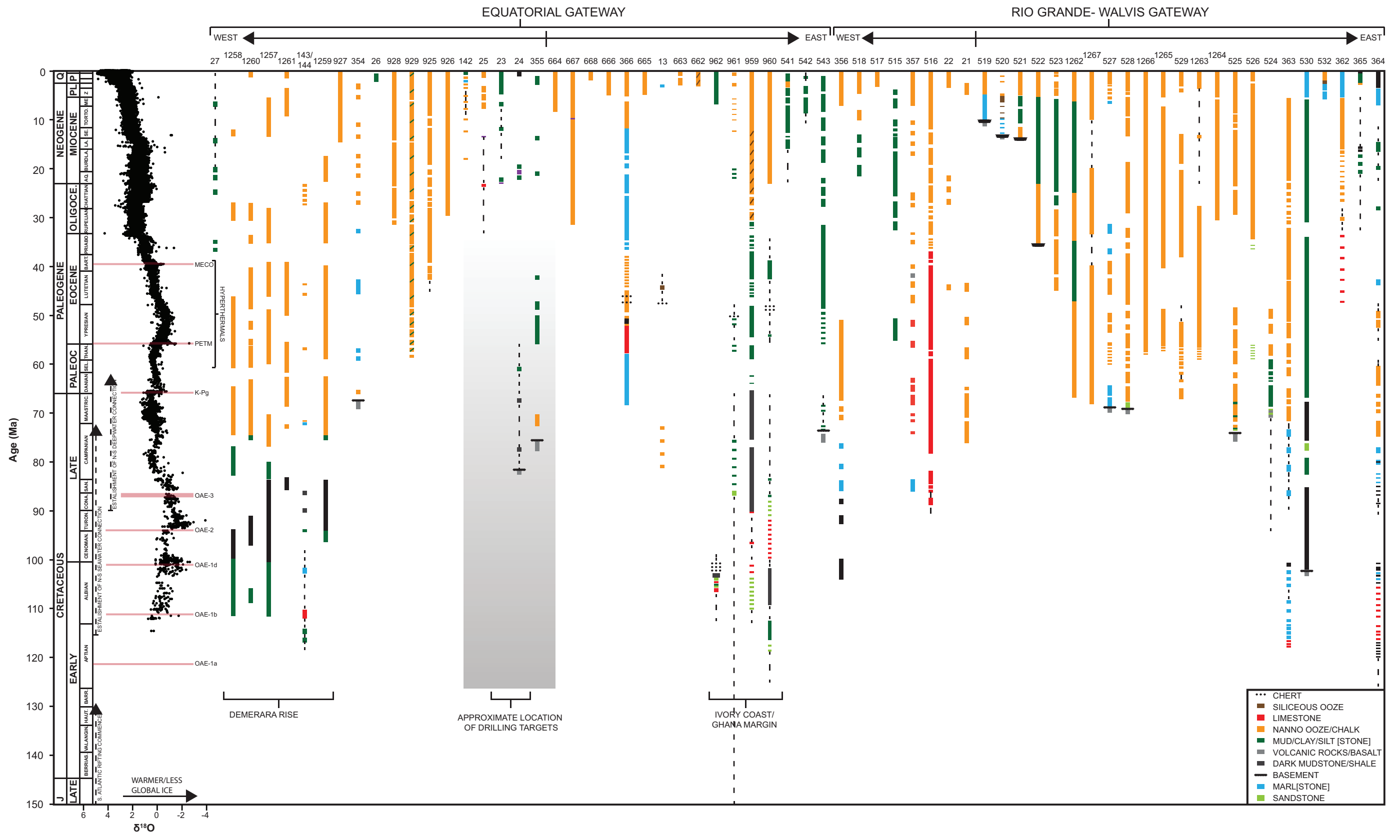

Figure F5. Interpolated, open access, single beam bathymetric data across the plateau region with location of BrasilSpan 2-D and CGG 3-D seismic reflection data and proposed drill sites. GH= Gaibu High; IH= Itamaracá High.

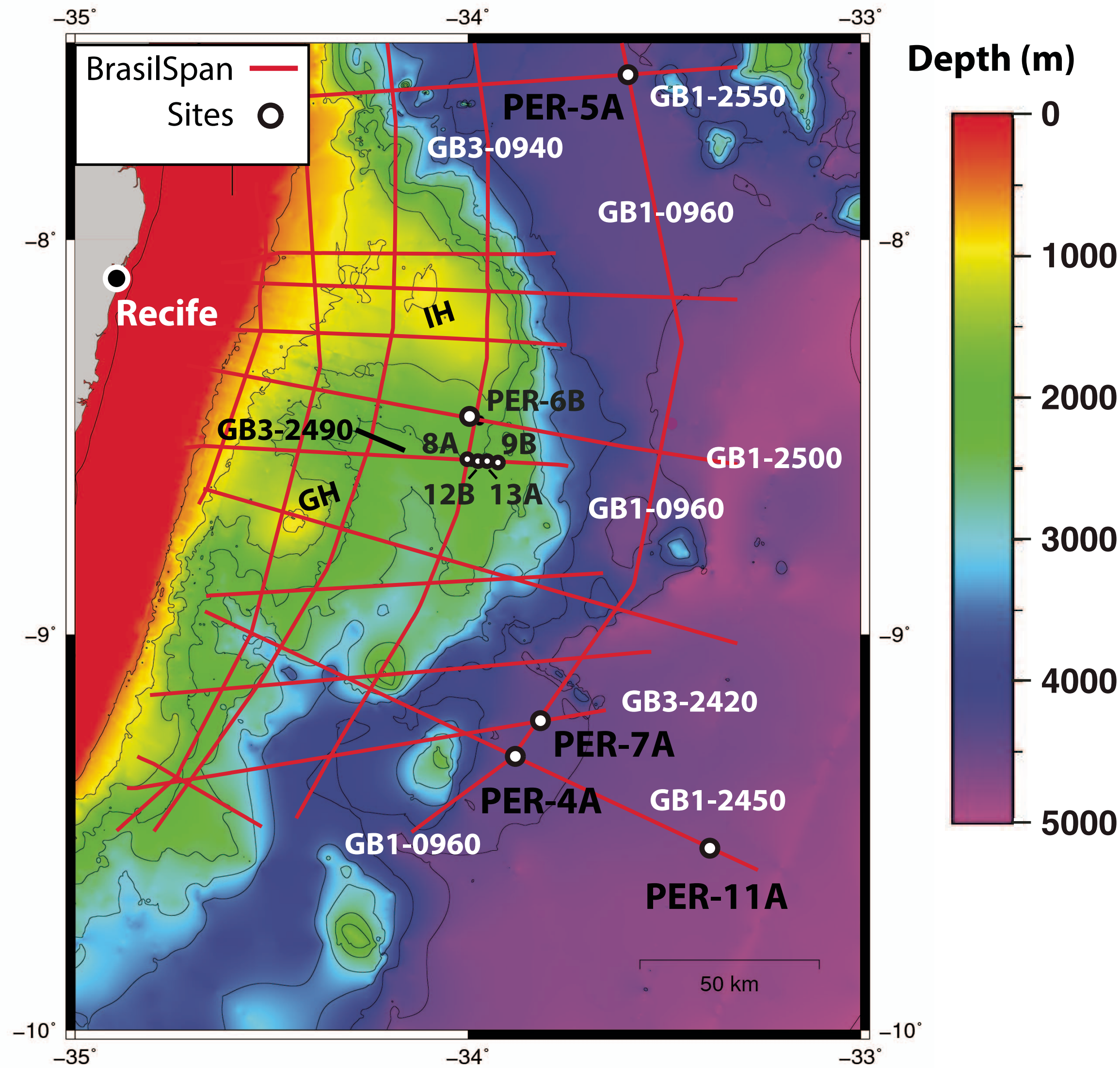

Figure F6. Gravity surveys and basement architecture. A. Free-air gravity from ship-towed data. B. Bouguer gravity using the interpolated bathymetry of Figure F3. Panels A and B are from Pérez-Díaz and Eagles (2017b) C. Depth to basement with major normal fault polygons; continent–ocean transition (COT) marked.

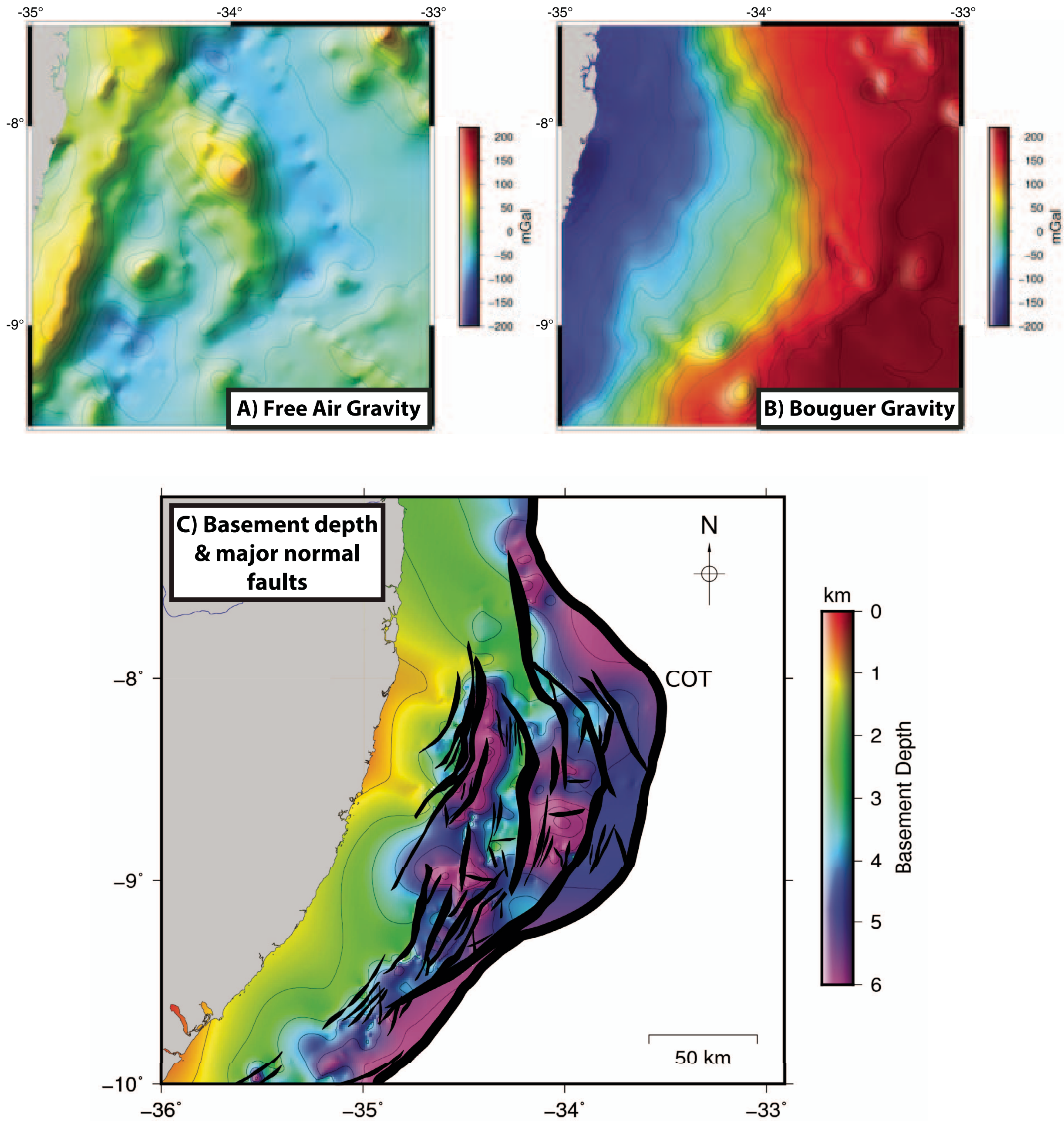

Figure F7. Modeled paleobathymetry of equatorial Atlantic rift system at 100 Ma of (A) Pérez-Díaz and Eagles (2017a) and (B) Müller et al. (2008). (C) Differences in subsidence history with different assumed breakup ages, based on the GDH-1 cooling model for oceanic lithosphere (Crosby et al., 2006). A ~20 My difference in oceanic crust age results in ~1500 m additional bathymetry at 100 Ma. Diff = depth differential resulting from 20 My age difference.

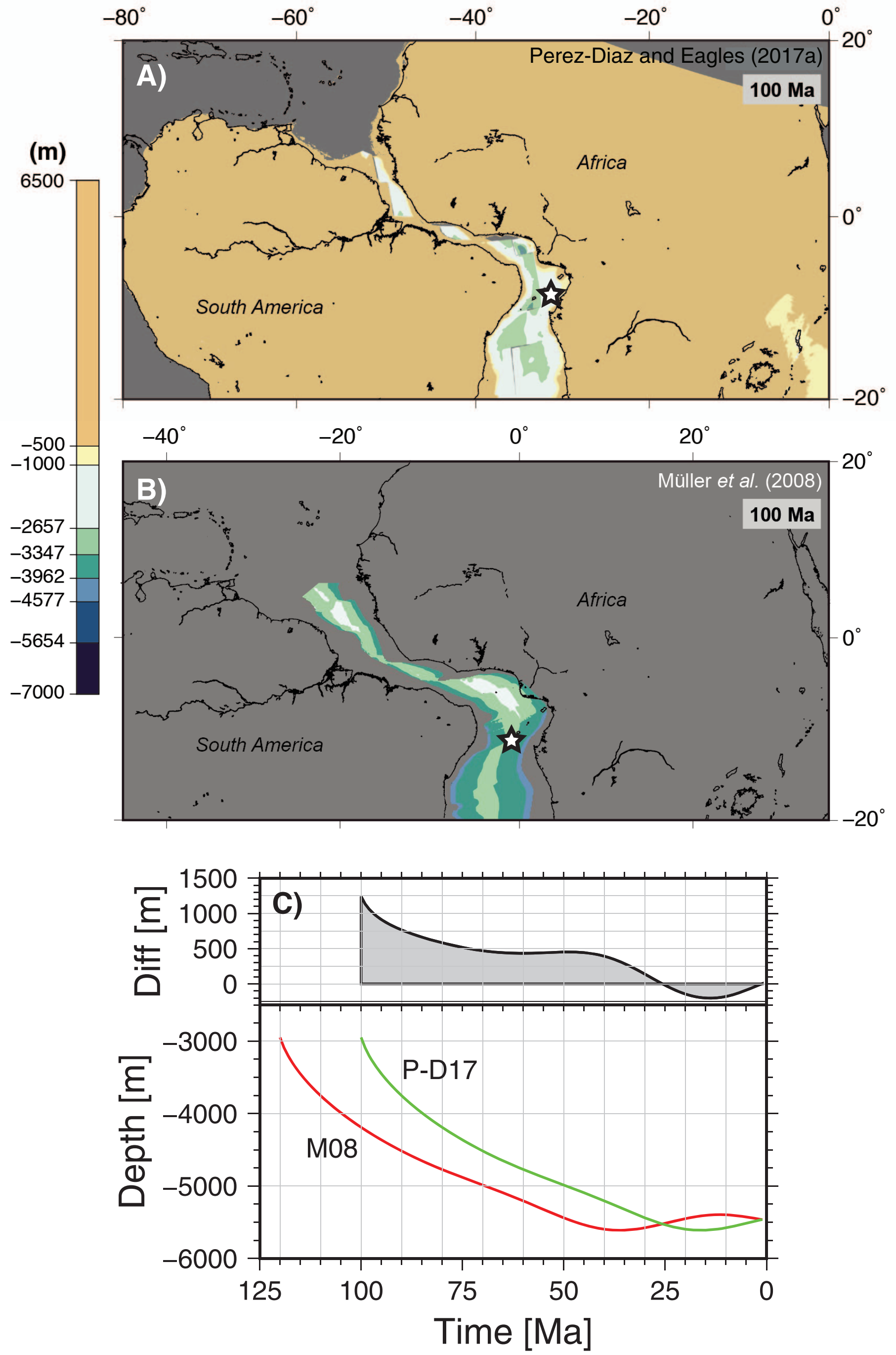

Figure F8. Summary of Cretaceous–Cenozoic environmental change, drill site depth evolution, and key science objectives. A. Expedition objectives and tectonic events. B. Depth evolution of drill sites located on and off the Pernambuco Plateau, illustrating the differential depth sampling possible through most of the Late Cretaceous–Cenozoic. C. Water mass evolution based on neodymium isotopic ratios with North/South Atlantic homogenization in the early Cenozoic (Voigt et al., 2013). D. Long-term benthic foraminiferal oxygen isotope stack (Friedrich et al., 2012; Zachos et al., 2001). Bottom panels: HadCM3L model climate simulations only forced by changing paleogeographic configuration (no change in greenhouse gas forcing), demonstrating the effect of EAG opening on cooling regional tropical climate (Lunt et al., 2016). Eq. = Equatorial. OAE = ocean anoxic event, K-Pg = Cretaceous/Paleogene boundary, PETM = Paleocene–Eocene Thermal Maximum, MECO = mid-Eocene Climate Optimum.

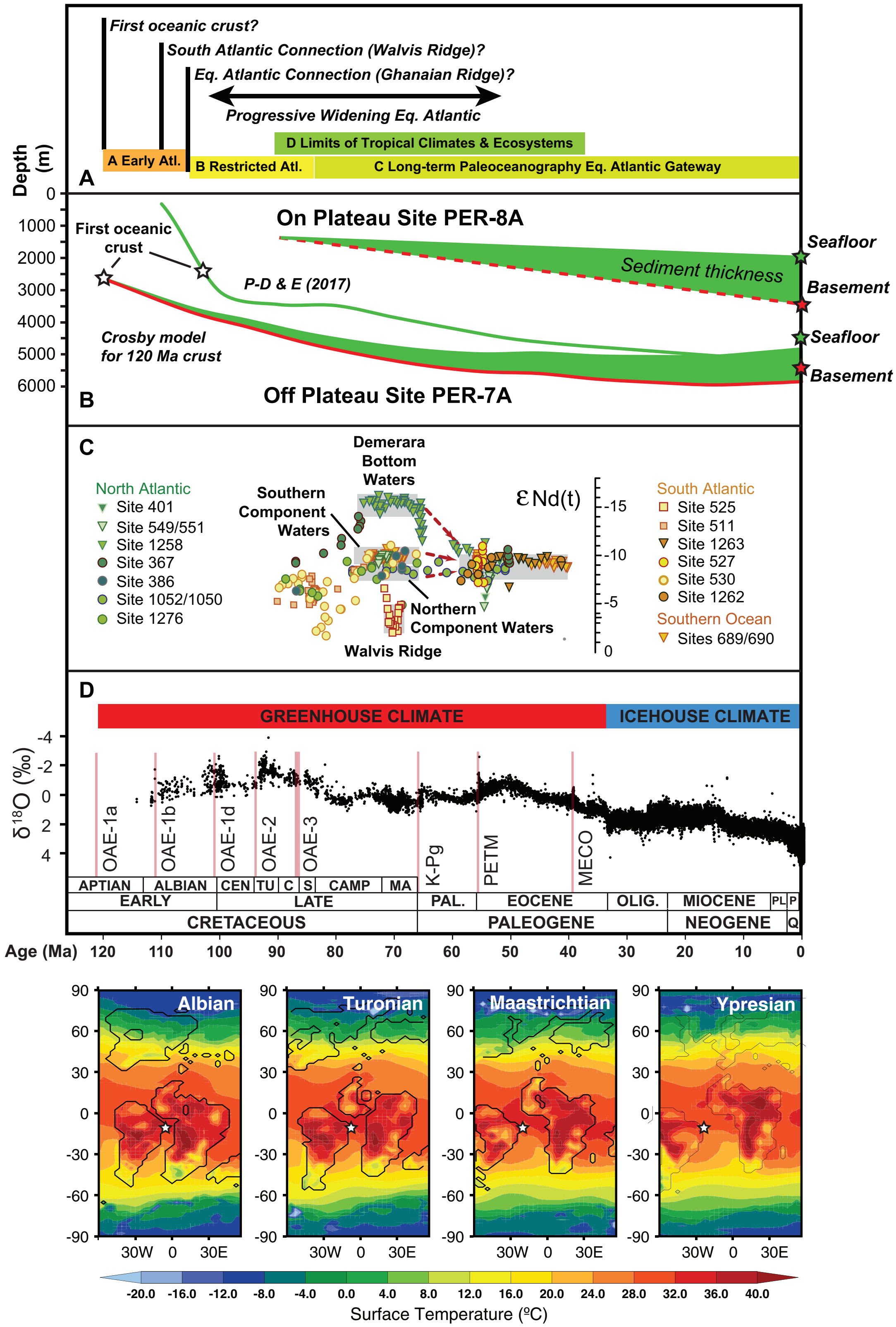

Figure F9. Model-data reconstruction of marine biogeochemistry before and during OAE2. (A, B) Seafloor oxygen condition showing modeled oxygen concentration in color. Gray contour = modeled oxygen concentration of 10 mmol O_2 l^{-1}, delimiting the region of seafloor dysoxia/anoxia. (C, D) Photic zone free hydrogen sulfide (H_2S) condition showing modeled H_2S concentration in color for 80–200 m depth. Euxinia is defined by the occurrence of free hydrogen sulfide ($H_2S > 0$, in white). Note focus of euxinia in the equatorial and South Atlantic (Monteiro et al., 2012).

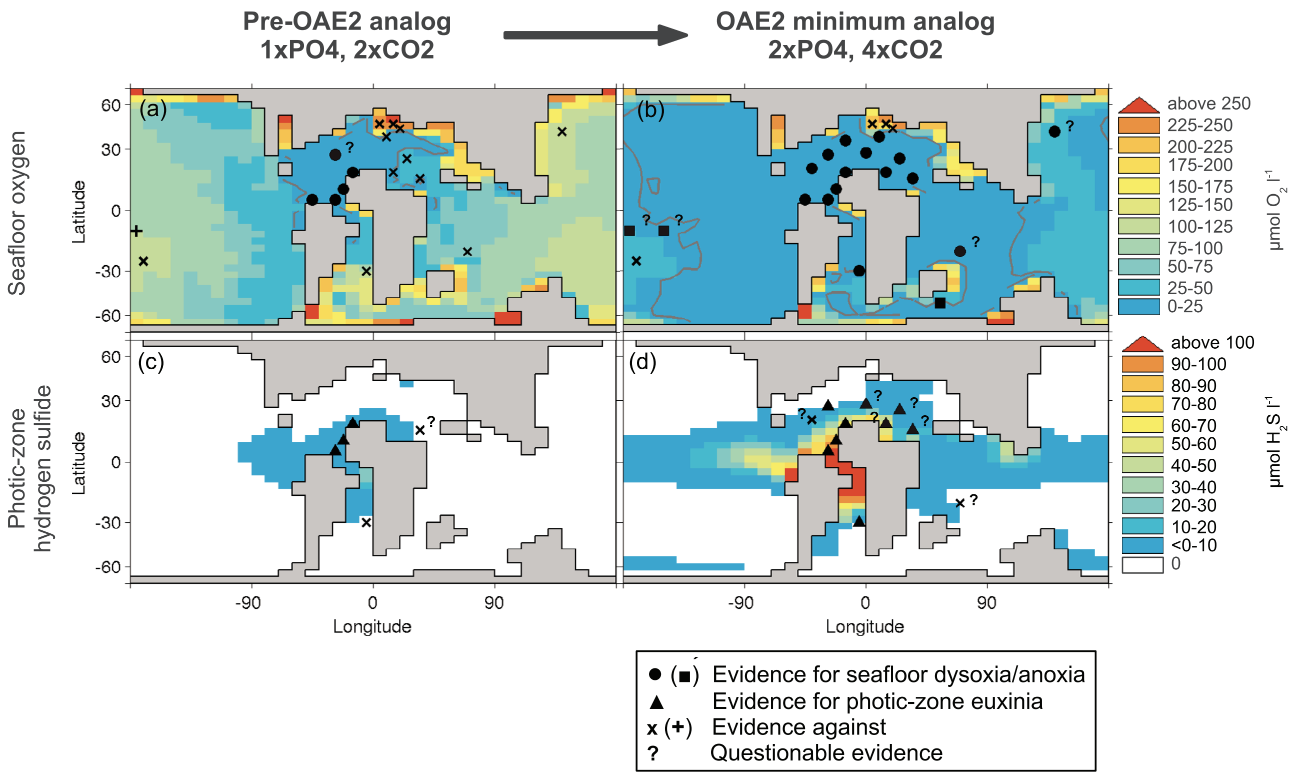

Figure F10. Core-top calcium carbonate contents for the equatorial South Atlantic (latitude 0° to 20° S) taken from Archer (1996), plotted as (A) a function of depth and (B) color coded by longitude. Red line = depth of Site PER-4A; larger outlined symbols = sites nearest to Site PER-4A. Light blue shading = region with sediments <10% $CaCO_3$. In B, yellow dots = nearest constraints to proposed drilling sites with $CaCO_3$ in weight percent.

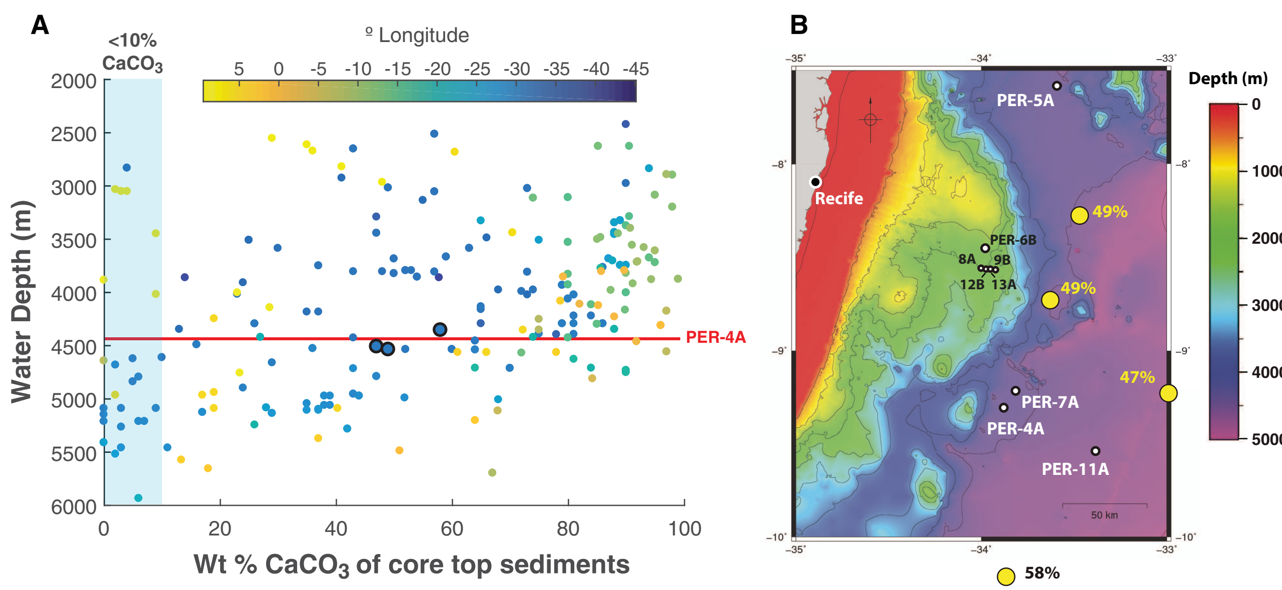

Site summaries

Site PER-4A

Priority:	Primary
Position:	9°18.9600′S, 33°52.3680′W
Water depth (m):	4441
Target drilling depth (mbsf):	999
Approved maximum penetration (mbsf):	1200
Survey coverage (track map; seismic profile):	Bathymetric sketch and site track map (Figure **AF1**) Deep-penetration seismic reflection: • Primary line: GB1-2450; SP 12234 (Figure **AF1**) • Crossing line: GB1-0960; SP 77175 (Figure **AF1**)
Objective(s):	• Recovery of oceanic basement; paleoenvironments of early postrift systems • Long-term paleoceanography of the equatorial Atlantic
Drilling program:	• Hole A - APC/XCB coring to refusal (~600 mbsf) • Hole B - APC/XCB coring to refusal (~600 mbsf) • Hole C - Reentry installation - drill-in 10.75" casing with HRT • Hole C - RCB coring from 400 mbsf to 999 mbsf
Logging/downhole measurements program:	• Hole B - logging with triple combo, FMS-sonic • Hole C - logging with triple combo, FMS-sonic, and VSI
Nature of rock anticipated:	Clay-rich hemipelagic and pelagic ooze; potential silts and sands in early postrift environments; basaltic oceanic crust

Site PER-5A

Priority:	Alternate
Position:	7°34.7940′S, 33°34.6020′W
Water depth (m):	4413
Target drilling depth (mbsf):	947
Approved maximum penetration (mbsf):	1150
Survey coverage (track map; seismic profile):	Bathymetric sketch and site track map (Figure **AF2**) Deep-penetration seismic reflection: • Primary line: GB1-2550; SP 12862 (Figure **AF2**) • Crossing line: GB1-0960; SP 93608 (Figure **AF2**)
Objective(s):	• Recovery of seamount volcanic basement • Long-term paleoceanography of the equatorial Atlantic
Drilling program:	• Hole A - APC/XCB coring to 600 mbsf • Hole B - Reentry installation - drill-in 10.75" casing with HRT • Hole B - RCB coring from 600 to 947 mbsf
Logging/downhole measurements program:	• Hole B - logging with triple combo, FMS-sonic, and VSI
Nature of rock anticipated:	Clay-rich hemipelagic and pelagic ooze; basaltic volcanic basement

Site PER-6B

Priority:	Alternate to PER-09B
Position:	8°27.3138′S, 33°59.1720′W
Water depth (m):	1835
Target drilling depth (mbsf):	1228
Approved maximum penetration (mbsf):	1230
Survey coverage (track map; seismic profile):	Bathymetric sketch and site track map (Figure **AF3**) Deep-penetration seismic reflection: • Primary line: GB1-2500; SP 11050 (Figure **AF3**)
Objective(s):	Long-term paleoceanography of the equatorial Atlantic
Drilling program:	• Hole A - APC/XCB coring to refusal (~600 mbsf) • Hole B - Reentry installation - drill-in 10.75" casing with HRT • Hole B - RCB coring from 400 mbsf to 999 mbsf
Logging/downhole measurements program:	• Hole B - logging with triple combo, FMS-sonic, and VSI
Nature of rock anticipated:	Clay-rich hemipelagic and pelagic ooze; basaltic volcanic basement

Site PER-7A

Priority:	Alternate to PER-04A
Position:	9°13.9020′S, 33°48.8160′W
Water depth (m):	4412
Target drilling depth (mbsf):	1015
Approved maximum penetration (mbsf):	1100
Survey coverage (track map; seismic profile):	Bathymetric sketch and site track map (Figure **AF4**) Deep-penetration seismic reflection: • Primary line: GB3-2420; SP 14352 (Figure **AF4**) • Crossing line: GB1-0960; SP 78110 (Figure **AF4**)
Objective(s):	• Recovery of oceanic basement • Paleoenvironments of early postrift systems • Long-term paleoceanography of the equatorial Atlantic
Drilling program:	• Hole A - APC/XCB coring to refusal (~400 mbsf) • Hole B - Reentry installation - drill-in 10.75" casing with HRT • Hole B - RCB coring from 400 mbsf to 1015 mbsf
Logging/downhole measurements program:	• Hole B - logging with triple combo, FMS-sonic, and VSI
Nature of rock anticipated:	Clay-rich hemipelagic and pelagic ooze; potential silts and sands in early postrift environments; basaltic oceanic crust

Site PER-8A

Priority:	Alternate
Position:	8°33.7500′S 33°59.4240′W
Water depth (m):	2003
Target drilling depth (mbsf):	400
Approved maximum penetration (mbsf):	400
Survey coverage (track map; seismic profile):	Bathymetric sketch and site track map (Figure **AF5**) Deep-penetration seismic reflection: • Primary line: GB3-2490; SP 11301 (Figure **AF5**) • Crossing line: GB3-0940; SP 13581 (Figure **AF5**)
Objective(s):	Cenozoic paleoceanography of the equatorial Atlantic
Drilling program:	• Hole A - APC/XCB coring to 400 mbsf • Hole B - APC/XCB coring to 400 mbsf • Hole C - APC/XCB coring to 400 mbsf
Logging/downhole measurements program:	• Hole C - logging with triple combo, FMS-sonic, and VSI
Nature of rock anticipated:	Clay-rich hemipelagic ooze

Site PER-9B

Priority:	Primary
Position:	8°33.7620′S 33°55.2660′W
Water depth (m):	2288
Target drilling depth (mbsf):	650
Approved maximum penetration (mbsf):	650
Survey coverage (track map; seismic profile):	Bathymetric sketch and site track map (Figure **AF6**) Deep-penetration seismic reflection: • Primary line: GB3-2490; SP 11920 (Figure **AF6**)
Objective(s):	• Recovery of volcanic basement • Long-term paleoceanography of the equatorial Atlantic
Drilling program:	• Hole A - APC/XCB coring to 590 mbsf • Hole B - APC/XCB coring to 590 mbsf • Hole C - Drill ahead to 575 mbsf; RCB core to 650 mbsf
Logging/downhole measurements program:	• Hole C - logging with triple combo, FMS-sonic, and VSI
Nature of rock anticipated:	Clay-rich hemipelagic and pelagic ooze; basaltic volcanic basement

Site PER-11A

Priority:	Alternate to PER-04A
Position:	9°32.4780′S 33°23.0040′W
Water depth (m):	4704
Target drilling depth (mbsf):	1000
Approved maximum penetration (mbsf):	1000
Survey coverage (track map; seismic profile):	Bathymetric sketch and site track map (Figure **AF7**) Deep-penetration seismic reflection: • Primary line: GB1-2450; SP 16979 (Figure **AF7**)
Objective(s):	Long-term paleoceanography of the equatorial Atlantic
Drilling program:	• Hole A - APC/XCB coring to refusal (~800 mbsf) • Hole B - Reentry installation - drill-in 10.75" casing with HRT • Hole B - RCB coring to 1000 mbsf
Logging/downhole measurements program:	• Hole B - logging with triple combo, FMS-sonic, and VSI
Nature of rock anticipated:	Clay-rich hemipelagic and pelagic ooze

Site PER-12B

Priority:	Primary
Position:	8°33.6000′S 33°58.4280′W
Water depth (m):	2047
Target drilling depth (mbsf):	400
Approved maximum penetration (mbsf):	400
Survey coverage (track map; seismic profile):	Bathymetric sketch and site track map (Figure **AF8**) Deep-penetration seismic reflection: • Primary line: GB3-2490; SP 11438 (Figure **AF8**)
Objective(s):	Cenozoic paleoceanography of the equatorial Atlantic
Drilling program:	• Hole A - APC/XCB coring to 400 mbsf • Hole B - APC/XCB coring to 400 mbsf • Hole C - APC/XCB coring to 400 mbsf
Logging/downhole measurements program:	• Hole C - logging with triple combo, FMS-sonic, and VSI
Nature of rock anticipated:	Clay-rich hemipelagic ooze

Site PER-13A

Priority:	Primary
Position:	8°33.9240′S 33°56.0940′W
Water depth (m):	2139
Target drilling depth (mbsf):	500
Approved maximum penetration (mbsf):	500
Survey coverage (track map; seismic profile):	Bathymetric sketch and site track map (Figure **AF9**) Deep-penetration seismic reflection: • Primary line: GB3-2490; SP 11790 (Figure **AF9**)
Objective(s):	Cenozoic paleoceanography of the equatorial Atlantic
Drilling program:	• Hole A - APC/XCB coring to 500 mbsf • Hole B - APC/XCB coring to 500 mbsf • Hole C - APC/XCB coring to 500 mbsf
Logging/downhole measurements program:	• Hole C - logging with triple combo, FMS-sonic, and VSI
Nature of rock anticipated:	Clay-rich hemipelagic ooze

Figure AF1. Bathymetry and seismic reflection lines, proposed Site PER-4A.

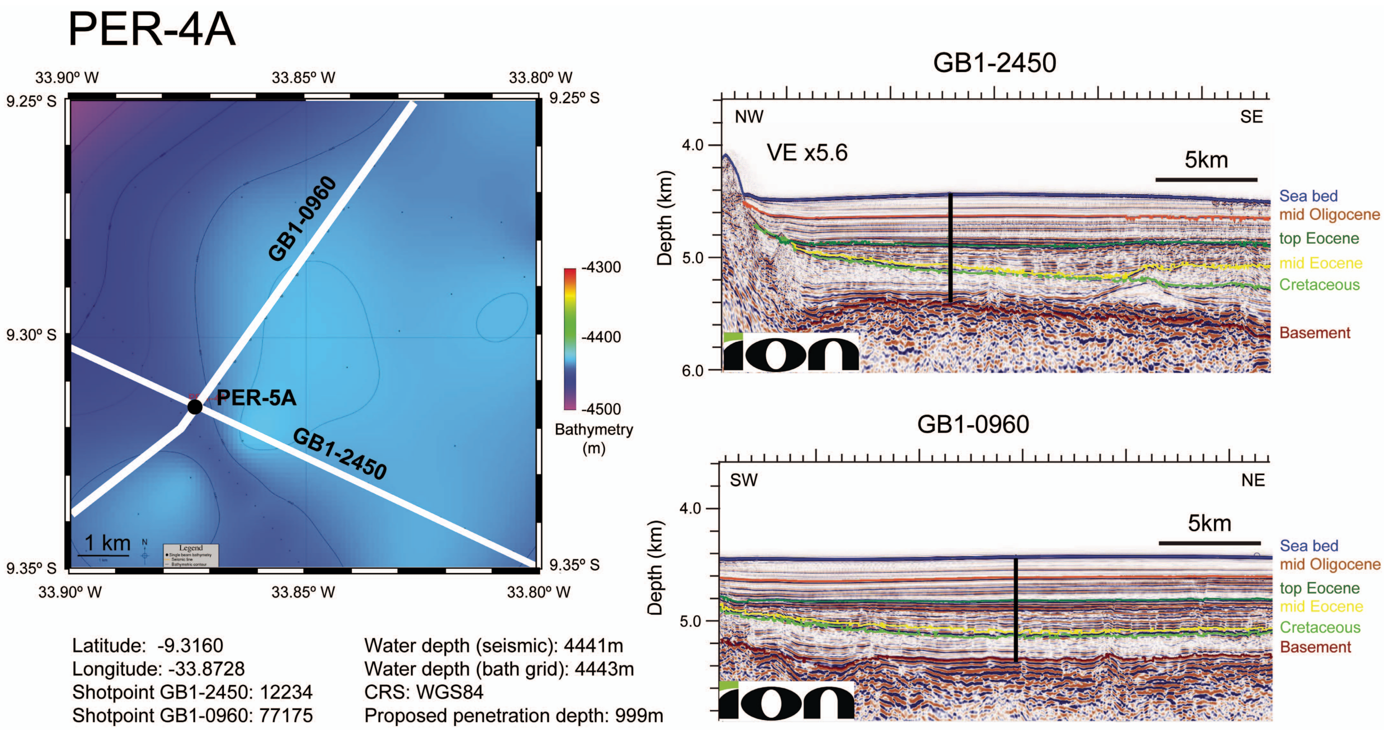

Figure AF2. Bathymetry and seismic reflection lines, proposed Site PER-5A.

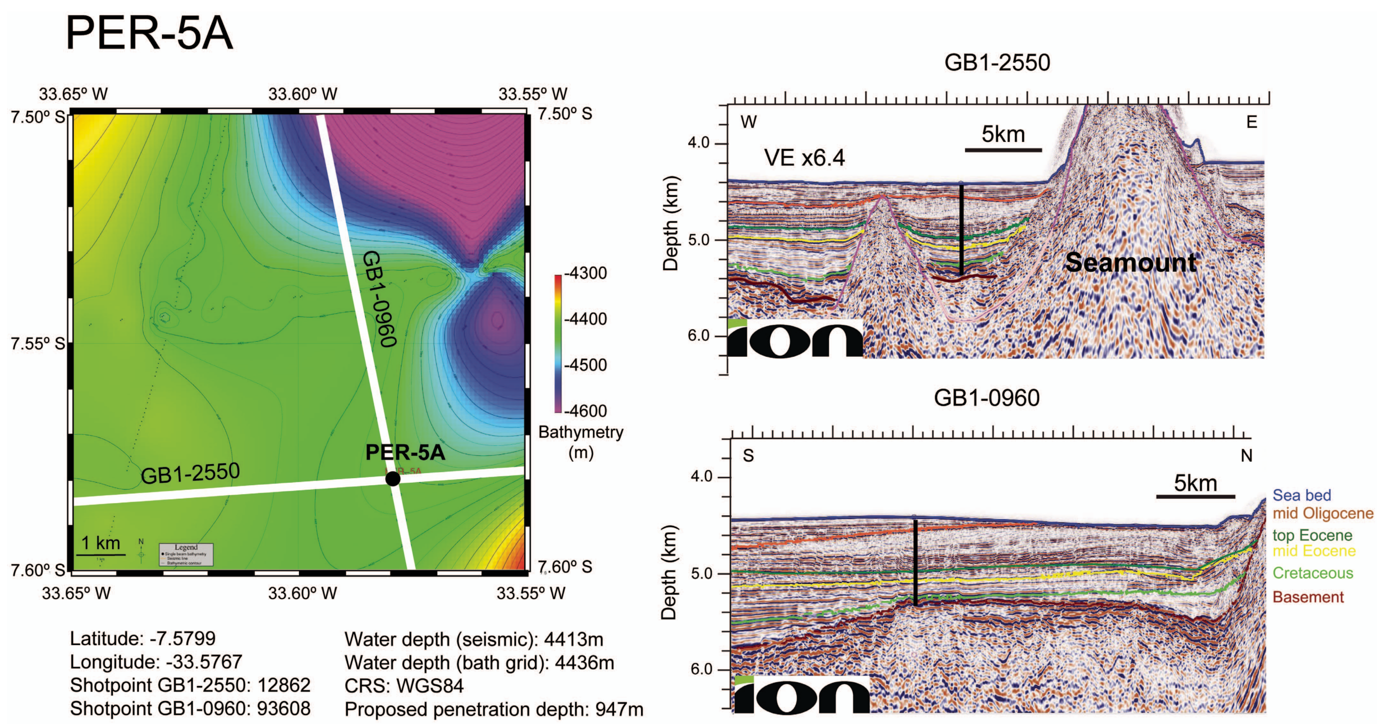

Figure AF3. Bathymetry and seismic reflection line, proposed Site PER-6B.

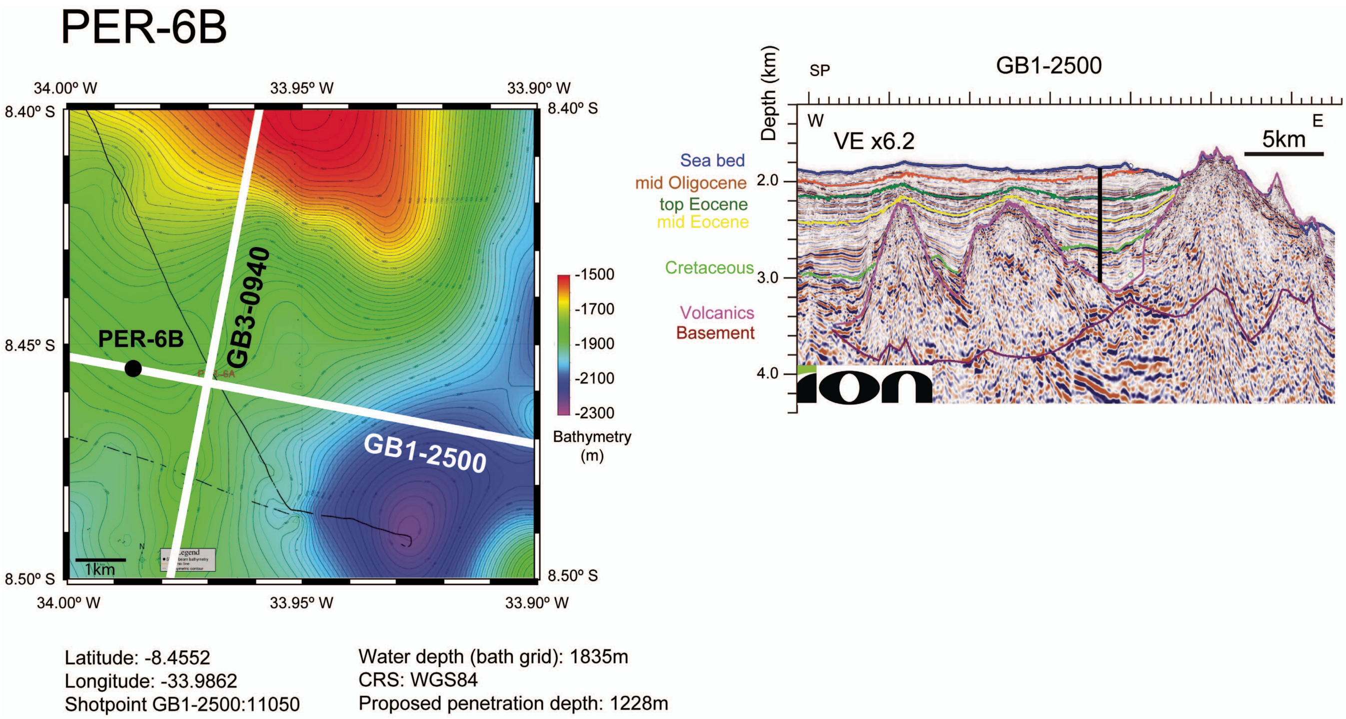

Figure AF4. Bathymetry and seismic reflection lines, proposed Site PER-7A.

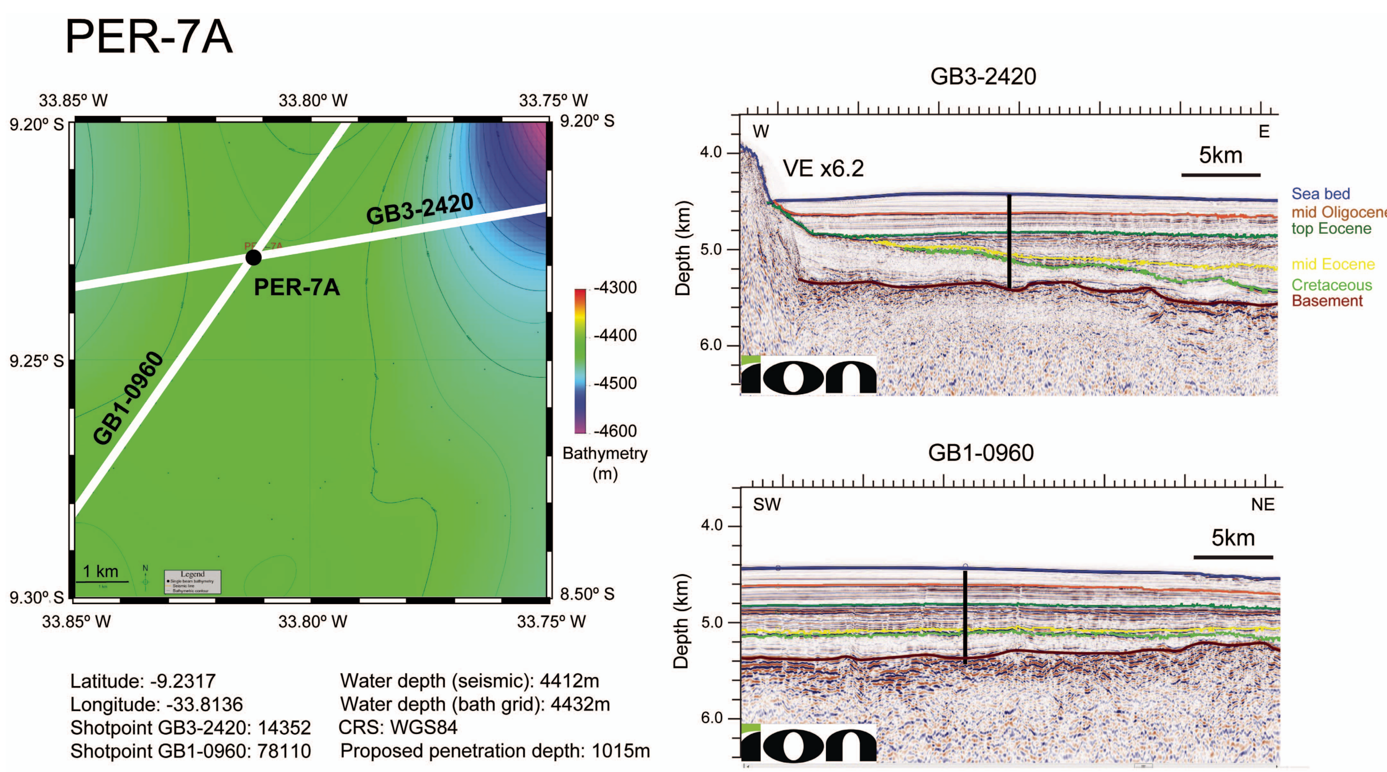

Figure AF5. Bathymetry and seismic reflection lines, proposed Site PER-8A.

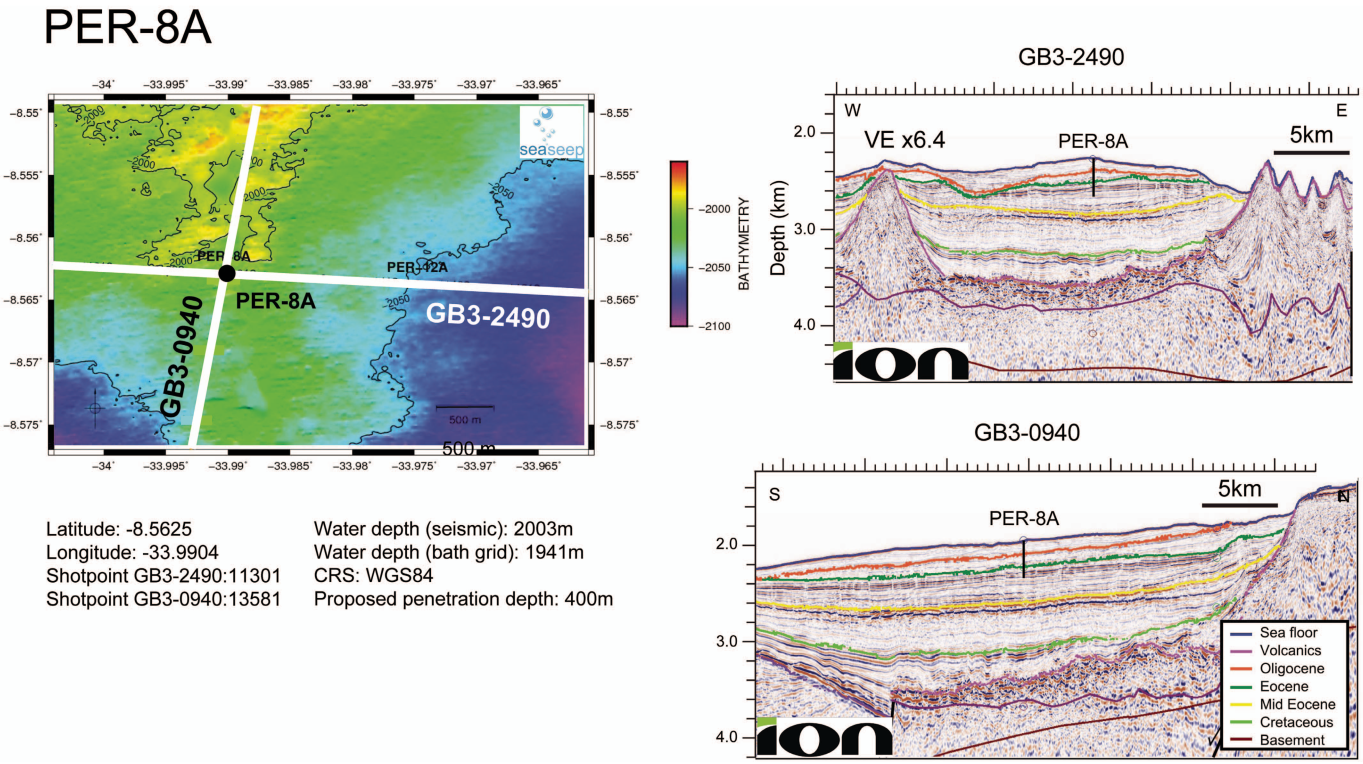

Figure AF6. Bathymetry and seismic reflection line, proposed Site PER-9B.

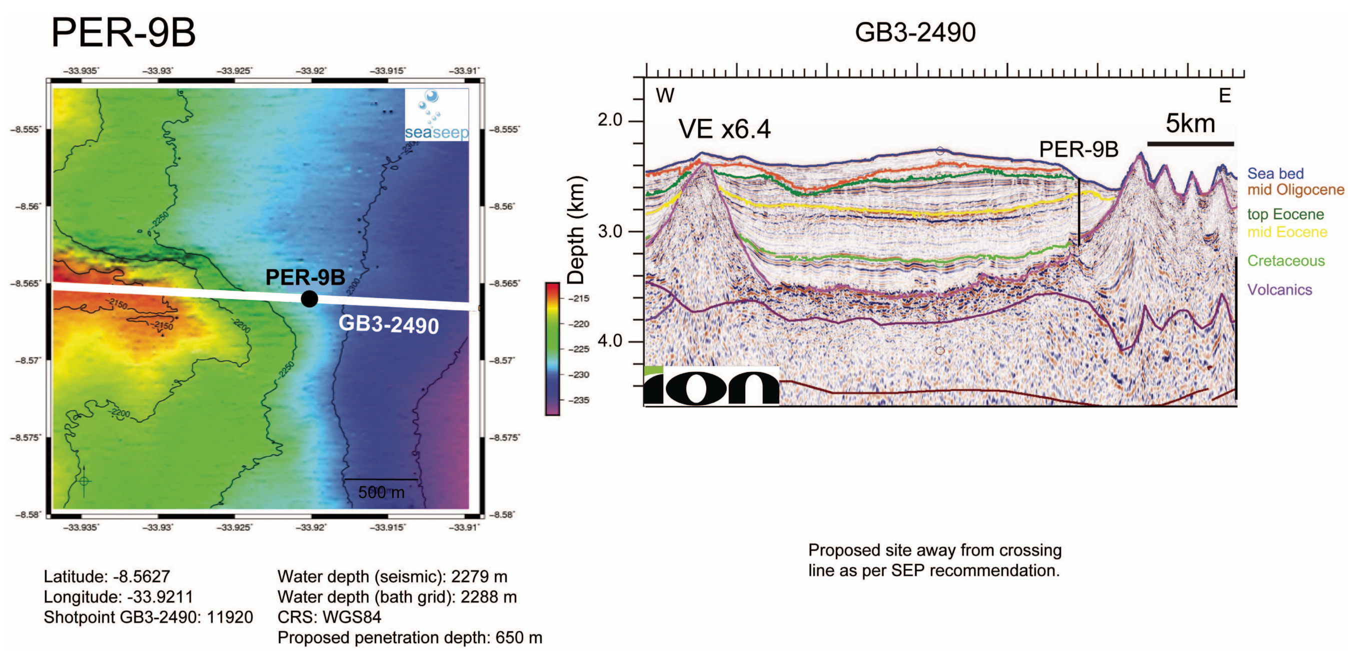

Figure AF7. Bathymetry and seismic reflection line, proposed Site PER-11A.

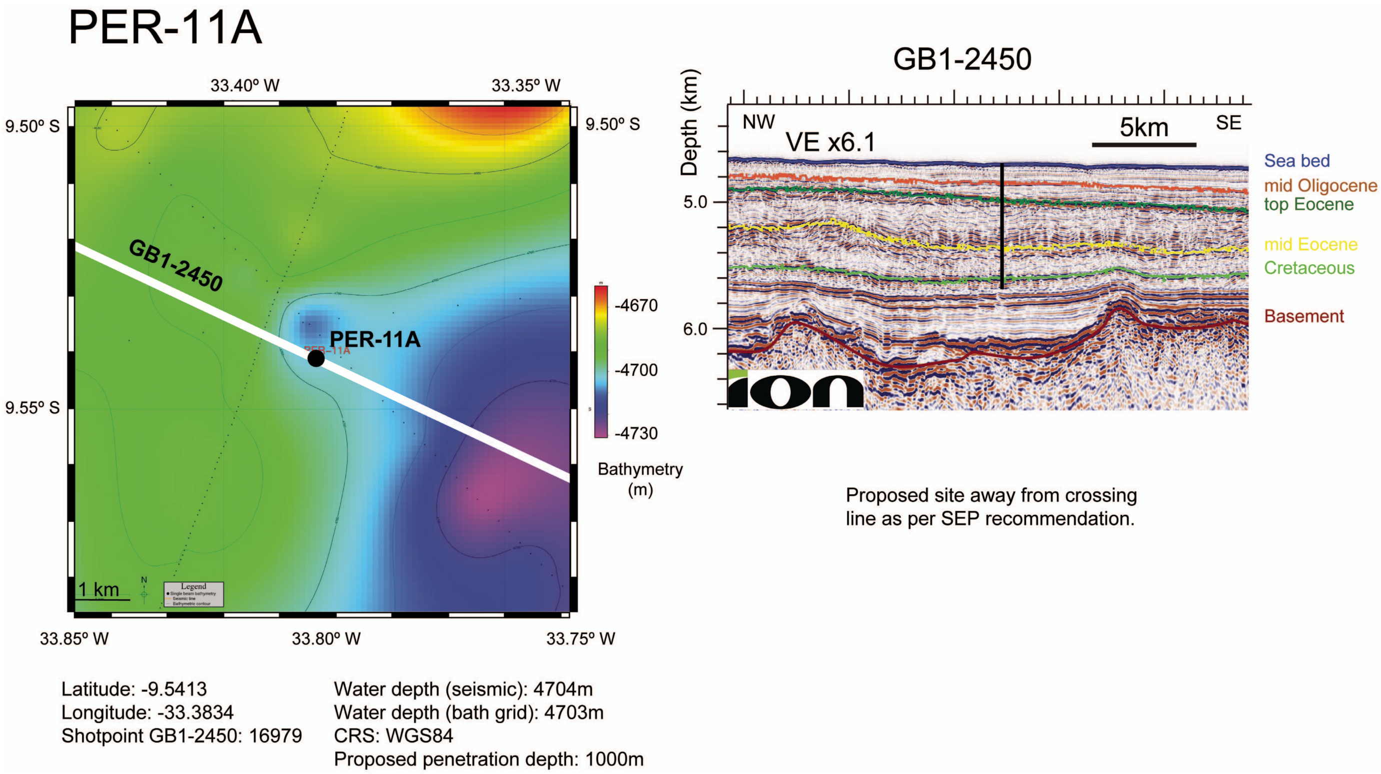

Figure AF8. Bathymetry and seismic reflection line, proposed Site PER-12B.

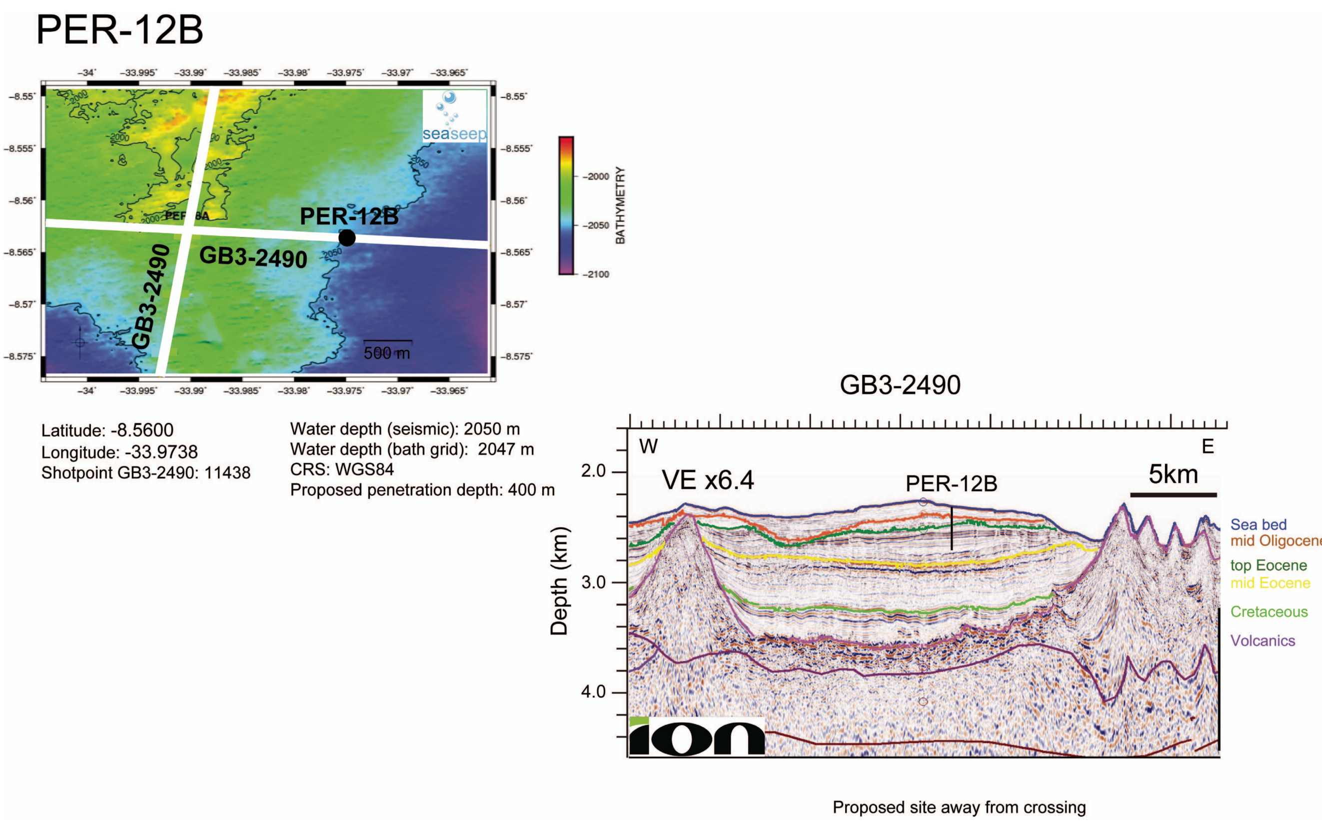

Figure AF9. Bathymetry and seismic reflection line, proposed Site PER-13A.